NOTICE
This report was prepared as an account of work sponsored by the United States Government. Neither the United States nor the United States Energy Research and Development Administration, nor any of their employees, nor any of their contractors, subcontractors, or their employees, makes any warranty, express or implied, or assumes any legal liability or responsibility for the accuracy, completeness or usefulness of any information, apparatus, product or process disclosed, or represents that its use would not infringe privately owned rights.

MECHANICAL PROPERTIES OF NON-METALLIC THIN FILMS

R. W. Hoffman

Professor Department of Physics

Case Western Reserve University - Cleveland, Ohio 44106

ABSTRACT

The importance of the mechanical properties, and especially the stress developed as a result of deposition processes and thermal treatment, is demonstrated by significant changes in many properties, in mass transport, and failure. In this review we first define the stress system, including non-uniform stress distributions and interfacial stresses. Different measurement techniques are compared and the restrictions on the elastic bending equations developed for the most common geometries.

Available data for elements, compounds, and glasses is catalogued and examined for systematic trends. Growth and crazing patterns can also supply qualitative information. The concepts which have been successful in detailing the origin of intrinsic stress in metals are briefly treated. The additional complications arising from the sensitivity to stoichometry and residual gas or other contaminations are discussed before attempting to develop models for the stress in non-metallic films. Quantitative successes of stress models are few at present. The relevance of the internal stress to failure modes is illustrated by three examples: enhanced mass transport, loss of adhesion, and fracture.

DISTRIBUTION OF THIS DOCUMENT IS UNLIMITED

DISCLAIMER

This report was prepared as an account of work sponsored by an agency of the United States Government. Neither the United States Government nor any agency Thereof, nor any of their employees, makes any warranty, express or implied, or assumes any legal liability or responsibility for the accuracy, completeness, or usefulness of any information, apparatus, product, or process disclosed, or represents that its use would not infringe privately owned rights. Reference herein to any specific commercial product, process, or service by trade name, trademark, manufacturer, or otherwise does not necessarily constitute or imply its endorsement, recommendation, or favoring by the United States Government or any agency thereof. The views and opinions of authors expressed herein do not necessarily state or reflect those of the United States Government or any agency thereof.

DISCLAIMER

Portions of this document may be illegible in electronic image products. Images are produced from the best available original document.

This report was prepared as an account of Government-sponsored work. Neither the United States, nor the Atomic Energy Commission, nor any person acting on behalf of the Commission:

A. Makes any warranty or representation, expressed or implied, with respect to the accuracy, completeness, or usefulness of the information contained in this report, or that the use of any information, apparatus, method, or process disclosed in this report may not infringe privately owned rights; or

B. Assumes any liabilities with respect to the use of, or for damages resulting from the use of, any information, apparatus, method, or process disclosed in this report.

As used in the above, "person acting on behalf of the Commission" includes any employee or contractor of the Commission, or employee of such contractor, to the extent that such employee or contractor of the Commission, or employee of such contractor prepares, disseminates, or provides access to any information pursuant to his employment or contract with the Commission, or his employment with such contractor.

SECTION I. INTRODUCTION

The importance of mechanical properties of thin films has been established over the past several decades. In the first place, many properties are substantially modified in a condensed film. The literature contains many examples[1] illustrating shifts in band-gap in semiconductors, transition temperature for superconducting films, or expected magnetic anisotropy. Any property which itself is strain sensitive, may well be modified in a deposited film. Even a property which is originally isotropic may have lower symmetry when the effects of the strain are considered. The control of the stresses by changing deposition conditions is one of the goals now partially reached in the search to develop new properties.

More recently, mechanical constraints introduced by the substrates have been used to produce or stabilize new film structures that are unknown in the bulk.[2] In this way properties or devices may be constructed that fit special needs and are unavailable by conventional techniques. This design, through the mechanical constraints in the system, is one of the more exciting new areas.

One of the earliest evidences of the importance of the mechanical properties is in the various modes of failure. These failures may be the more obvious ones of actual fracture of the film or buckling as a result of the loss of adhesion to the substrate. Dislocations or cracks may be introduced in the substrate at high stress levels. Somewhat more subtle effects such as strain-enhanced diffusion or electromigration may also occur.[3]

A complete review would define the stress and strain system, consider the techniques for measurement of the internal stress, as well as present the data and consider the various models for the origin of the stress. The tensile properties should also be treated, including the elastic modulus, the tensile strength, plastic deformation, and the fracture mode. Indeed, the earlier general reviews by Hoffman,[4,5] Campbell,[6,7] Buckel,[8] Kinosita,[9] Scheuerman,[10] and books,[11] have proceeded along these lines. We will not attempt to reproduce that which already exists in these review papers. We shall update them, however, and call attention to the more sepcialized reviews, especially in those areas where the information is pertinent to non-metallic films.

We also consider our task to discuss the stress and strain distributions found in a film so that a given property may, in turn, be calculated. New experimental techniques and data will, of course, be included.

Although at this time we begin to understand, at least in principle, the mechanical properties of metallic films, our state of knowledge for non-metallic films is much more rudimentary. In the first place, the properties seem to be not very reproduceable from laboratory to laboratory and, indeed, seem to depend sensitively on the conditions of deposition. In addition, instabilities or pronounced changes in the internal stress may be seen when compound films are exposed to the atmosphere or other surroundings after removal from the system. All of these make for a much more difficult problem in understanding the origin of the internal stress because the structure of non-metallic films is not so well characterized. We shall see that stoichiometry and rapid diffusion of ambient gasses are partially responsible. In spite of these difficulties, a qualitative understanding is emerging.

SECTION II. THE ELASTIC PROBLEM

Formulation of the Elastic Problem

Since, as we will see, the mechanical properties of a film on a substrate are primarily a result of constraints introduced by the substrate, we wish to understand both qualitatively and quantitatively the nature in which the forces are distributed in the film and substrates and then transmitted across their interface. Even though many problems of practical importance can be solved in terms of isotropic elasticity, we wish to set up the problem generally enough that we can consider cases of anisotropic strains. We must also take account of single crystal films and substrates in order to include epitaxial cases.

Only strains may be experimentally measured. Hence the stresses we talk about are calculated on the basis of measuring deformation, knowing the boundary conditions and assuming that the sample is in equilibrium. Following Nye[12] and Smith[13] we use a mutually orthogonal coordinate system with the x_1' and x_2' axes in the plane of the film and the x_3' axis normal to the film plane.

The coordinate system is defined in Fig. 1. The first subscript refers to the direction of the force on a face perpendicular to the second index. Thus, σ_{11}', σ_{22}' are the normal stresses in the plane and σ_{33}' is the normal stress perpendicular to the film plane. The shear stresses σ_{12}', σ_{23}', and σ_{31}' together with rotational equilibrium, represent force systems attempting to decrease the angle between the axes indicated. The corresponding normal strains are ε_{11}', ε_{22}' and ε_{33}' and shear stress ε_{12}', ε_{23}', ε_{31}. We point out that the tensor shear strains (ε's) are half the engineering shear strains (γ's) since the γ's represent the decrease in angle between two original orthogonal directions. The primes are used since the orthogonal primed axes are sample axes and are not the crystal (unprimed) axes.

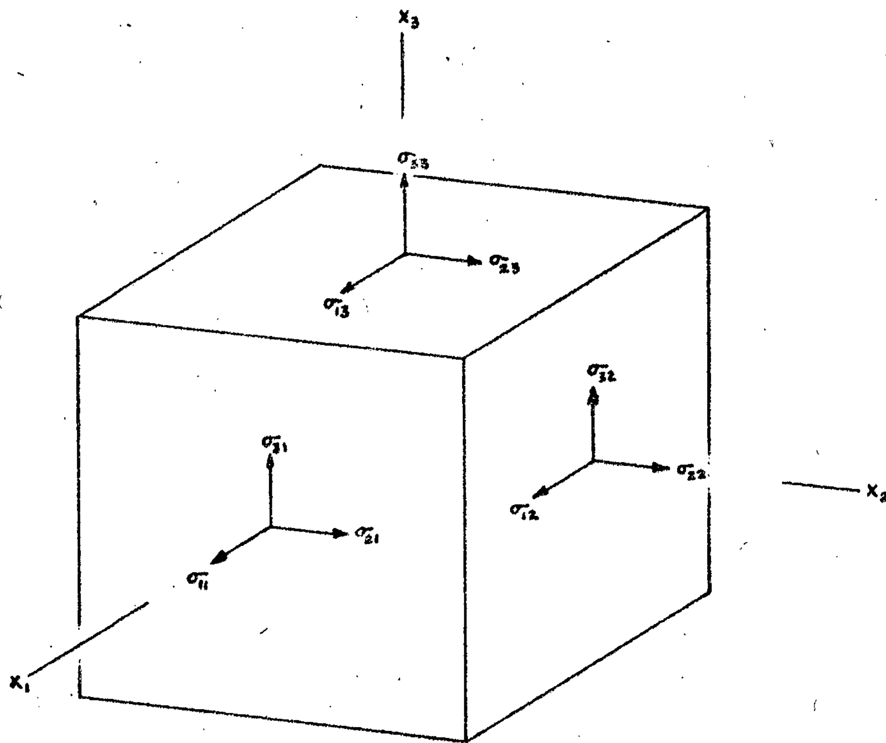

Figure 1. Definition of stress system.

Since elasticity is a fourth-rank tensor property,

$$\varepsilon'_{ij} = s'_{ijke}\ \sigma'_{ke}$$

and (1)

$$\sigma'_{ij} = c'_{ijke}\ \varepsilon'_{k\ell}$$

where the s's are the elastic compliances and the c's the stiffnesses for the particular sample orientation. Fourth rank tensor properties can be quite complex in the case of low symmetry crystals. The 81 possible components may be reduced by well-known equilibrium and symmetry arguments.

Even in the cubic system three constants are independent and two are needed for an isotropic specimen. The elastic equations are often reduced to the two index notation[12,13]

$$\varepsilon'_{i} = s'_{kj}\ \sigma'_{j} \qquad (2)$$

$$\sigma'_{i} = c'_{ij}\ \varepsilon'_{j}$$

where the subscripts 1, 2 and 3 stand for normal components and 4, 5, and 6 refer to the shear components for both stresses and strains. The reader is reminded that the arrays s_{ij} and c_{ij} are not second rank tensors in this notation.

For the (001) orientation in the cubic system, we may drop the primes and find the independent constants s_{11}, s_{12} and s_{44} or c_{11}, c_{12} and c_{44} listed in the handbooks. For a general orientation the primed constants must be calculated by transforming from the crystallographic axes where the elastic constants are tabulated to the primed sample axes. Nye, among others, gives this prescription.

Young's modulus defined as the ratio of the longitudinal stress to the longitudinal strain, i.e., $1/s'_{11}$, is often desired. For the cubic system[13]

$$\frac{1}{E_{\ell_i}} = s_{11}-2(s_{11}-s_{12} - \frac{1}{2} s_{44})(\ell_1^2\ell_2^2 + \ell_2^2\ell_3 + \ell_3^2\ell_1^2) \quad (3)$$

where $\ell_1\ell_2\ell_3$ are the direction cosines of the arbitrary direction ℓ_i referred to the crystallographic directions. As the quantity $(s_{11}-s_{12}-1/2\ s_{44})$ is positive for all cubic metals except molybdenum, Young's modulus has a maximum in <111> and a minimum in <100> directions. Young's modulus is independent of direction in the plane for (111) orientations. Nye lists expressions for Young's modulus for crystals of lower symmetry.

Vook and Witt[14] give expressions for Young's modulus in several simple directions. Turley and Sines,[15] following Thomas,[16] separate the given stiffness in a constant and orientation-dependent part and then suggest several rotation methods to calculate the transformation. Polar plots are given for several shear constants for Cu, Mo, and Si.

For convenience in our discussion and following equations, we will drop the primes from the notation. In order to obtain a better feeling for the problem, let us consider the simplifications of an isotropic elastic substrate. Firmly attached to this substrate is a film which is also elastically isotropic, We shall regard the dimensions in the plane as being semi-infinite. If we now consider a homogeneous stress in the film, and invoke the usual boundary conditions of no forces at the free surfaces or edges, we have the situation of Fig. 2, where we depict the forces acting on an interior section of the film. As we shall see later this corresponds in reality to the situation found in most systems except near the edges of the film itself, or perhaps at the boundaries of crystallites within the films. In this figure we see that the film is in a state of tensile stress indicated by the total force per unit width of the fim, F.

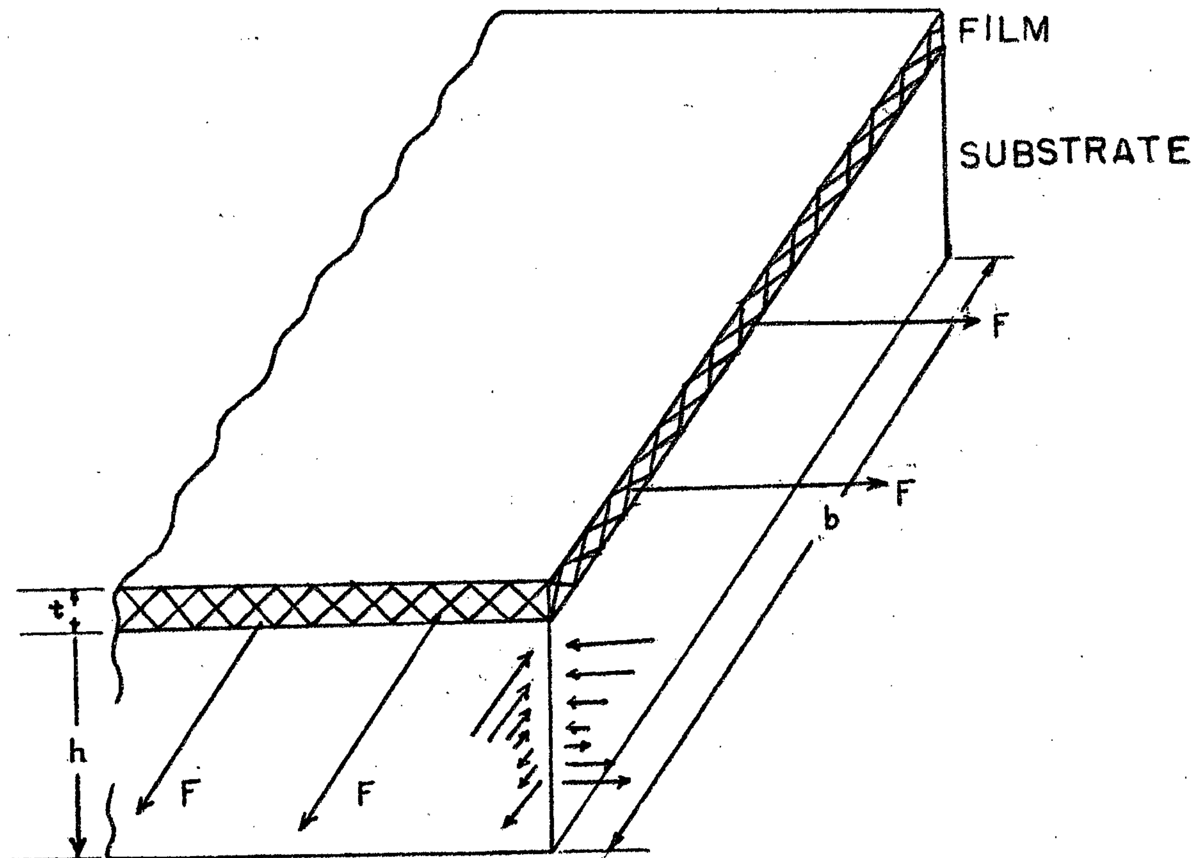

Figure 2. Forces acting on an interior section of the film-substrate composite.

We note that this tension is a biaxial one. As one traverses the interface in a direction normal to the plane of the film, there is a discontinuity in the stress but the strain is continuous. If the film is in tension we find that the substrate is in compression just below the interface.

In fact, if the film is quite thin compared to the substrate, the neutral plane is a third of the substrate thickness from its free surface.

Thus our oversimplified picture of a film under the uniform tensile strain would give us the situation indicated in Fig. 3. An interior volume element would see the normal stresses, σ_{11} and σ_{22} but no shear stresses. If we imagine cutting through the film in the center we see a uniform tensile stress, assuming the

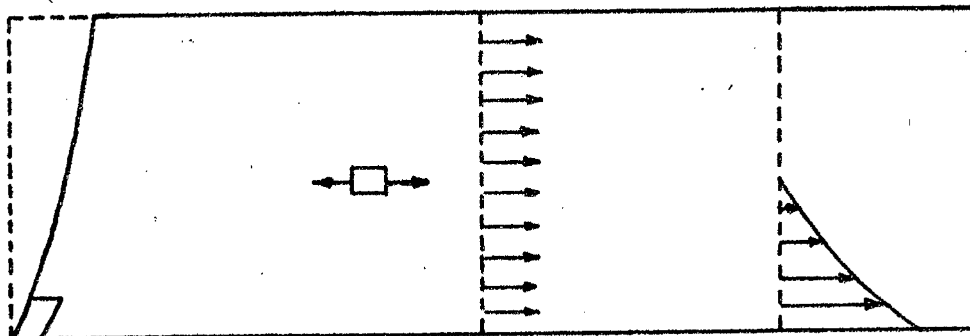

Figure 3. Idealized stress distributions within a constrained film.

substrate were rigid. If, on the other hand, the origin of stress were concentrated at the interface, we would see decreasing tensile forces as indicated schematically in the figure when we moved away from the interface. The free edges of the film can support no forces. Hence, as seen in the left hand side of the figure, we would expect shears to exist only near the edges of the film.

Stress Distribution

Let us consider some of these points in more detail. There are two problems that need to be attacked. One is the stress distribution within the interior of the substrate and film, and the second, the effects near the edges. We will consider the first of these. As pointed out by Brenner and Senderoff,[17] and treated in the review by Hoffman, using the case where the elastic constants of film and substrates are the same, and later extended by Doljack,[18] the problem is one of longitudinal forces in the film superposed on bending. It is instructive to look at each of these separately.

If we apply an external force to the composite plate longitudinally, so that all of the fibers strain equally, then the stresses across the cross section will be those indicated in Fig. 4 for the case of a biaxial stress system. A discontinuity in the stress exists at the interface but the stress in each of the substrate and the film is uniform.

In the case of pure bending, when only an external moment is applied to each of the elemental pieces and no external force is

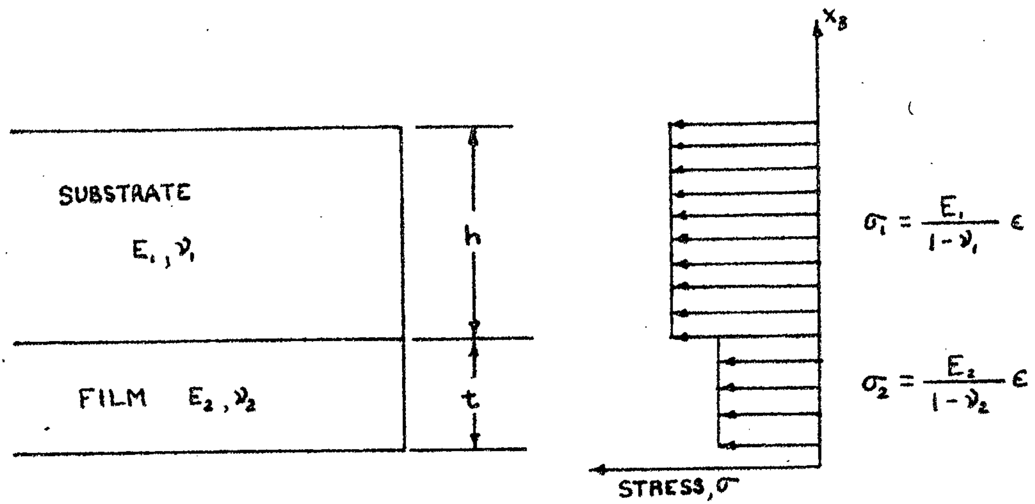

Figure 4. Stress distribution for longitudinal applied force.

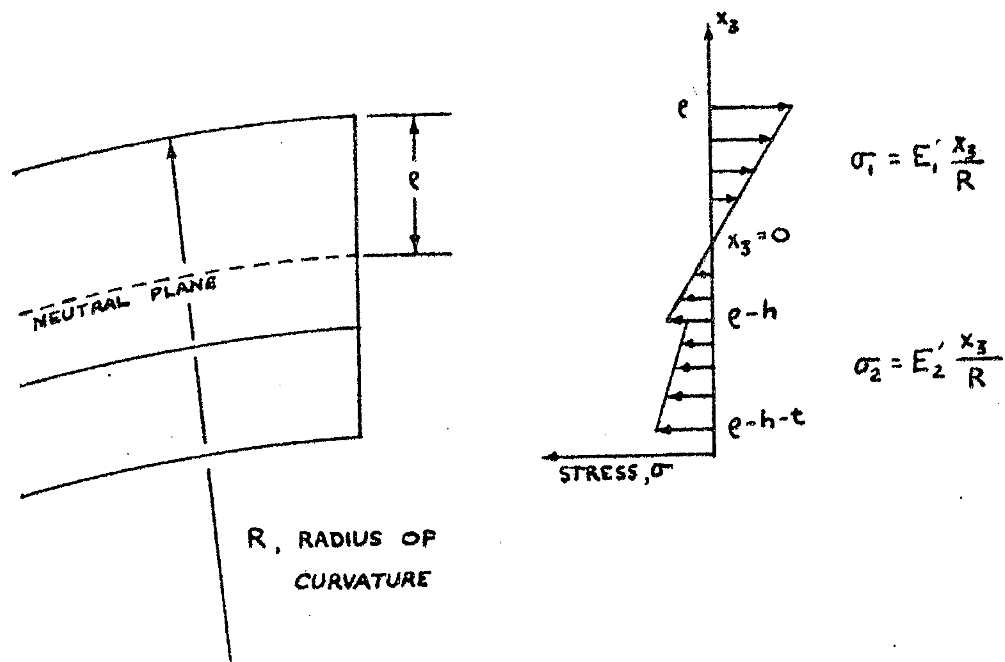

Figure 5. Stress distribution resulting from bending.

applied, the elastic response is only a bending strain. This produces the stress distribution as shown in Fig. 5. It is seen that the bending gives rise to non-uniform stress in the direction perpendicular to the film, arising from the fact that the stretching in the longitudinal fibers depends on the distance from the plane of zero bending strain. If the plate were not a composite one this plane of zero bending stress would just be in the middle.

We now relate these longitudinal and bending relaxations to the actual case of depositing a film on the substrate. Consider first a substrate clamped against bending and contraction during the deposition of the film. In this case the stress distribution in the film after deposition is the intrinsic stress. This distribution is indicated schematically in Fig. 6, and of course, the distribution of the stress need not be constant throughout the thickness of the film. The total force exerted by the film is the integral of the stress over the thickness of the film; and is equal to the product of the average stress and the film thickness

$$F = St = \int_{o}^{t} \sigma(t)dt \qquad (4)$$

where $\sigma(t)$ represents the stress distribution as a function of the thickness t.

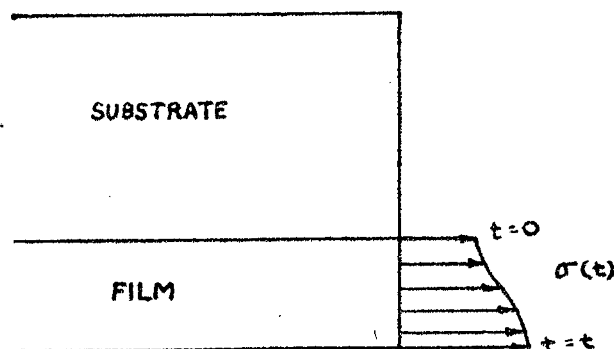

Figure 6. Intrinsic stress distribution for deposition with substrate clamped against bending and contraction.

If we now release the clamping preventing contraction, but still do not allow any bending to take place, the stress distribution throughout the plate is modified as in Fig. 7. The uniform stress distributions σ_1 and σ_2 are produced by the net contraction of the tensile stress distribution, $\sigma(t)$ in the film. The relaxed stress distribution in the film $\sigma'(t)$ is just the original distribution reduced by the constant stress σ_2. Equilibrium is achieved when the total force on the cross section depicted in Fig. 7, is zero.

If the remaining clamps are now removed and the plate is allowed to bend, it reaches an equilibrium radius of curvature. This bending of the film substrate plate gives rise to a relaxation of the stress as was indicated in our discussion of pure bending. In essence, the additional contraction which results from the necessity to achieve bending equilibrium decreases the actual stress in the film even more. And, furthermore, makes it non-uniform as a function of thickness. The radius of curvature may be determined by equating the moment of the film to the moment produced by the stresses resulting from the bending. The plane of zero elastic strain, or neutral plane, is now shifted, and may be determined from the condition that there is no net external force exerted across any cross-section and thus the sum of the bending forces must be zero.

Equations for the radius of curvature and the relieved stress distribution are given by Brenner and Senderoff[17] for the case of identical elastic constants of the film and substrate and Doljack[18] and Klokholm[19] for the general case. The stress distribution will be modified by a bending distribution as depicted in Fig. 4. If $\sigma(t)$ is constant, Klokholm calculates the relaxation correction M by which the simple Stoney[20] average stress S should be multiplied to obtain the true average stress.

$$M = \frac{\beta^3(\ +1)}{(\beta^3+\eta)(\beta+\eta) + 3\eta\beta(\beta+1)^2} \tag{5}$$

where β is the substrate to film thickness ratio h/t and η is the ratio of elastic constants $E_f/1-\nu_f$ and $E_s/1-\nu_s$. E is Young's modulus and ν Poisson's ratio. The subscripts f and s refer to film and substrate. For $b > 1000$ and any η or $b > 10$ and $\eta < 0.2$ N is sufficiently close to 1 to be experimentally negligible.

In practice it is difficult to clamp a substrate sufficiently well to meet both the conditions of no bending and no expansion during deposition. A much more common case is that with the substrate completely free during deposition. During deposition an initially flat plate begins to bend slightly relieving the stress in the film already deposited. The continuous bending proceeds, giving rise to a stress relief in the film in addition to the con-

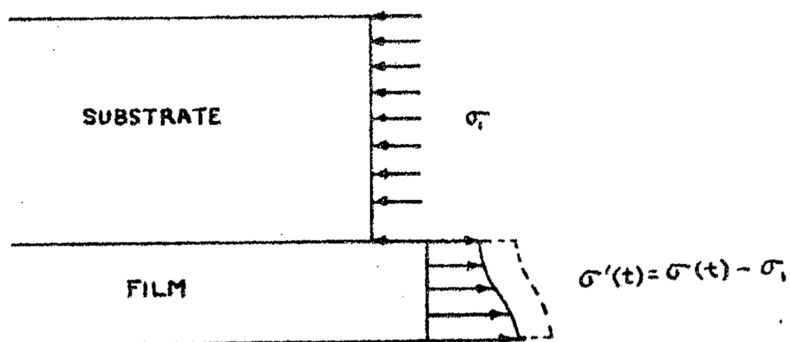

Figure 7. Relaxed stress distribution upon releasing longitudinal clamps.

traction and bending just discussed. Under these conditions the relief in each layer is different when the deposition is completed. If the mechanism giving rise to the stress in the first place were originally a process uniform with thickness then the result of such a stress relief would clearly give rise to larger stresses near the outside growing edge of the film as indicated in Fig. 8.

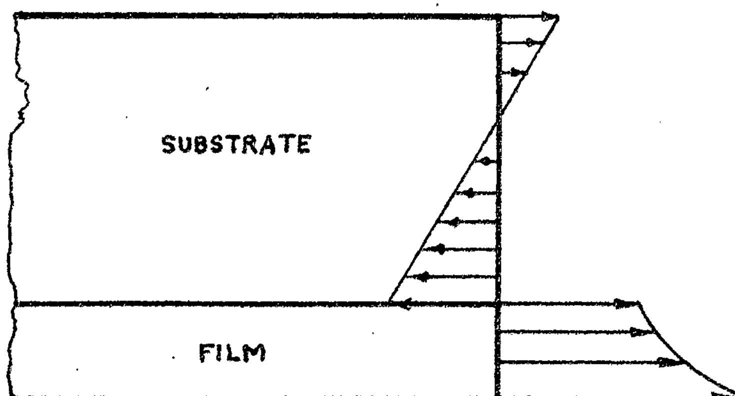

Figure 8. Relaxed stress distribution for free cantilevered substrate during deposition after Brenner and Senderoff.[17]

Brenner and Senderoff, suggested that this would be an explanation for the fact that many films curl when detached from the substrate in a way to suggest that the outer layer has the higher stress. Fortunately, these stress relief terms are not large in practical cases since the film is generally much, much thinner than the substrate. On the other hand, we must keep in mind that they will give rise to stress gradients within the film. The stress distributions have been calculated by the authors previously referenced, and the errors are less than the previous case for the same geometry.

Chaudhari[21] gives an approximate treatment of the relaxation following the thermal stress analysis of Timoshenko. The stress distribution in the film may be written as:

$$\sigma_{11} = \sigma_{22} = \frac{\varepsilon_{11}E}{1-\nu}\{1 - \frac{C}{D}[1+\frac{3(C-D)(x_3-D)}{D^2}]\} \quad . \qquad (6)$$

For this treatment ε_{11} is the assumed uniform strain arising from thermal contraction or other mechanism, E and ν are the usual elastic constants assumed the same for film and substrate, $C = t/2$, the film half-thickness, and $D = h+t/2$, the substrate plus film half thickness. x_3, the coordinate normal to the film, is 0 on the free surface of the film.

The first term in the equation represents the stress as one would calculate it considering a rigid substrate. The second term represents the contraction or compressional relaxation while the third term represents the bending relaxation. The stress distribution in the substrate is given by

$$\sigma_{11} = \sigma_{22} = \frac{\varepsilon_{11}E}{1-\nu}\frac{C}{D}[1+\frac{3(C-D)(X_3-D)}{D^2}] \quad . \qquad (7)$$

The results are presented in Fig. 9 for several values of C/D. As the stress in the substrate is reduced by the factor C/D, it is obvious that in most cases of deposition the film is much, much thinner than the substrate so that the stress in the substrate is only a very small fraction of the stress in the film. If we consider a film thickness of 1 μm and a substrate thickness of 1 mm, than the maximum value of the stress in the substrate is less than 1/2% of the stress in the film.

As Chaudhari has pointed out the critical feature of whether plastic flow will take place in the substrate is the value of critical resolved shear stress. If the stress in the film is 1% of the shear modulus and we consider the case where the ratio of

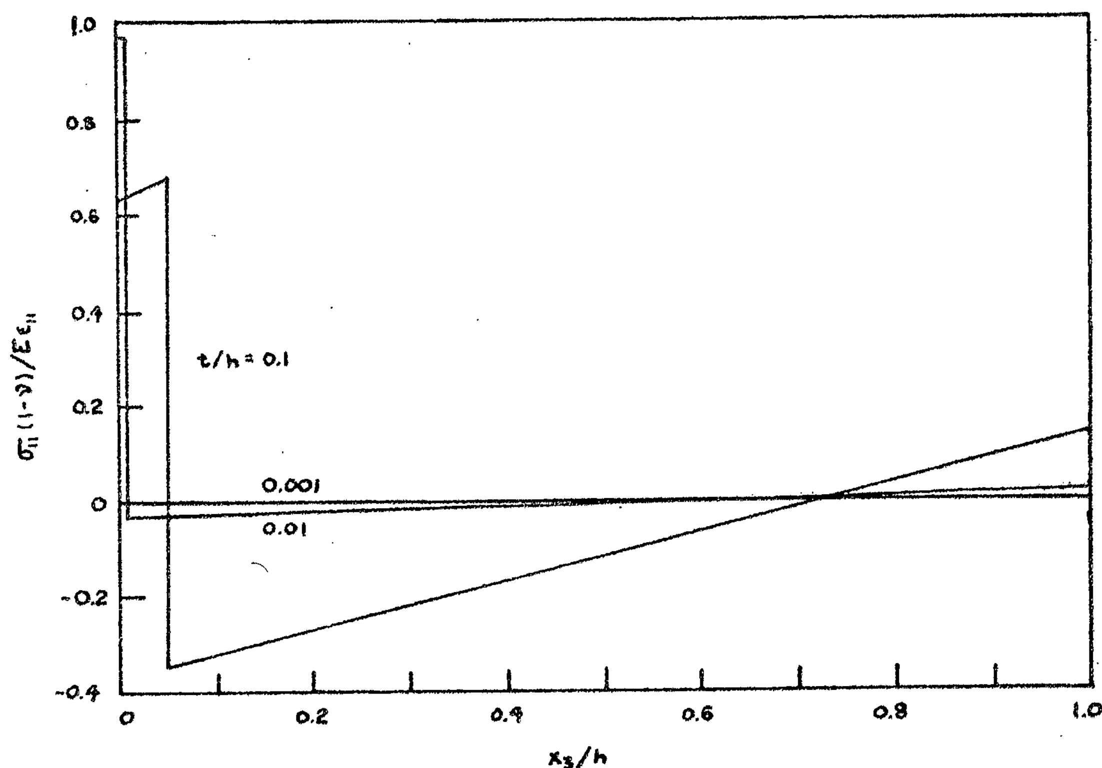

Figure 9. Approximate stress distribution for several values of film-substrate thickness ratio. After Chaudhari.[21]

the film thickness to the substrate thickness is 10^{-4}, the maximum value of stress in the substrate would be 10^{-6} μ. For comparison, most bulk single crystals will begin to undergo a plastic deformation when the shear stress is of the order of 10^{-5} or 10^{-4} times the shear modulus μ. Thus, when the film thickness is very thin, compared to the substrate thickness, we can neglect plastic flow by a dislocation mechanism in the substrate. When the ratio of the film thickness to the substrate thickness is larger than 10^{-4} we have to consider the particular substrate in question to determine whether or not plastic flow may take place.

There are two cases of practical importance where one has to be concerned about plastic deformation in the substrate. One of these, of course, is the obvious one where the material in the substrate is such that it easily undergoes plastic deformation, alkali halides for instance. Stress concentrations at propagating crack tips may also introduce dislocations in single crystal

substrates. Dislocations and other local defects may also be introduced in the substrate during growth. The second case takes place when the substrate is comparable to the film in thickness. As one can see by examination of Fig. 9, the relaxation in the film and substrate is sufficient to cause a non-uniform stress distribution within the film as well.

Similar distributions have been calculated by Oel and Frechett[22] for both large and small area planar interfaces for the case of comparable film and substrate thicknesses. Model experiments with thermal strains induced in birefiringent glasses gave good agreement with the calculations except when diffusion took place during sealing at high temperatures. In this case, far from merely smoothing the stress gradient, diffusion-caused stresses had large effects in magnitude and even sign of the stresses.

No detailed treatment concerning the sharpness of the interface seems to exist. The large stress gradient in this region may play a role in interfacial dislocation generation or mass flow and other effects, and represents an area of needed future study.

Edge Effects

We now consider the second part of the question, namely, the spatial details of the stress distribution. Of course, if the mechanism giving rise to the stress in the first place is not uniform, then the stress distribution will be non-uniform as well. Such distributions will be discussed later under origins of the intrinsic stress. However, we shall consider here the case where we initially have a large stress $\sigma_{11} = \sigma_{22}$ that lies in the plane of the film, is isotropic, and nearly uniform throughout the thickness, and is uniform over most of the area of the film. If we look at the cross section of the film-substrate composite, we see that the film appears to be a rectangular plate attached along its long edge to what we shall assume to be a semi-infinite rigid substrate. As a result, a slab of thin film attached to the substrate is under a state of stress nearly identical to that of a rectangular plate clamped along an edge and having undergone thermal expansion.

This latter problem has been treated approximately by Aleck.[23] We shall consider the question of thermal expansion later, but at the moment, we shall use the results of this treatment to ask the question as to the stress distribution near the edges of the film. According to Aleck, the problem is first converted to one of boundary tractions. The film is detached from the substrate and allowed to relax. To bring it back to a uniform state of stress, one imagines applying a uniform stress of magnitude σ_i normal to the ends of the film as shown in the top of Fig. 10. Next, the film

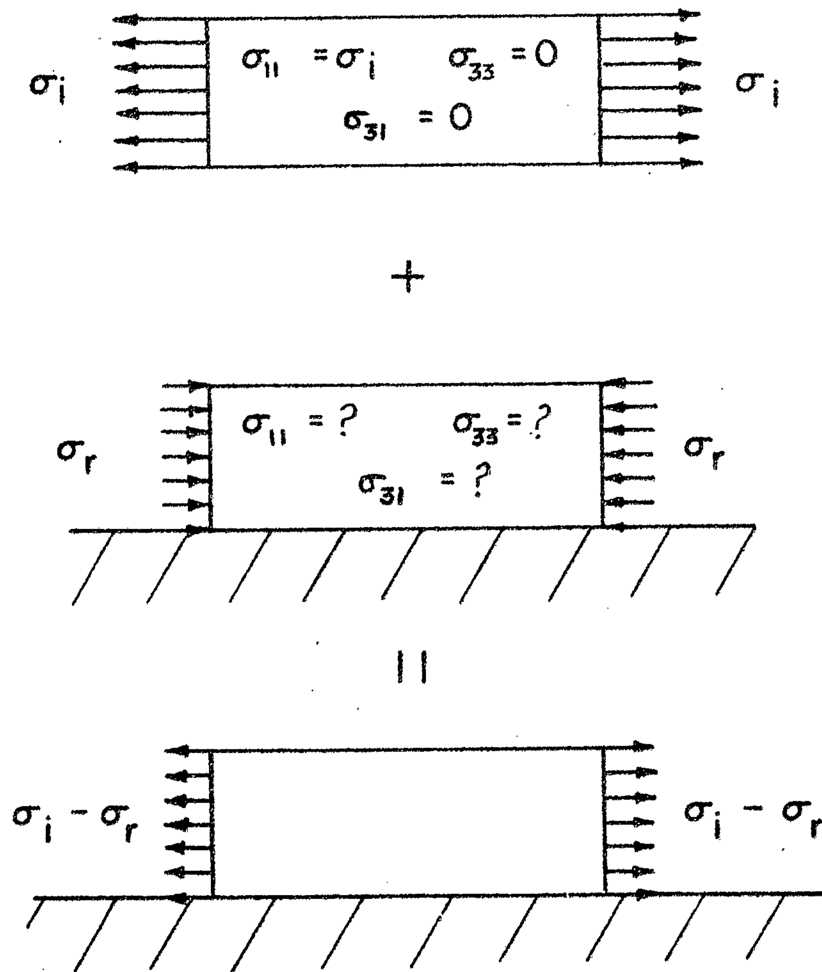

Figure 10. Boundary traction method applied to a thin film under uniform intrinsic stress constrained to a rigid substrate. After Aleck[23] modified by Doljack.[18]

is attached to the substrate and a uniform compressive stress σ_r is applied to its ends. σ_r in this case is equal to σ_i because at the edge of the film there are no net applied normal boundary tractions. The solution to the problem of the specified surface traction thus replaces the original stress problem. Doljack has solved this problem based on the approximate solution of Aleck for the case of thickness of the film being much thinner than its length. Fig. 11 shows the results of these calculations. The pertinent pictures are these: σ_{11} is just equal to the intrinsic

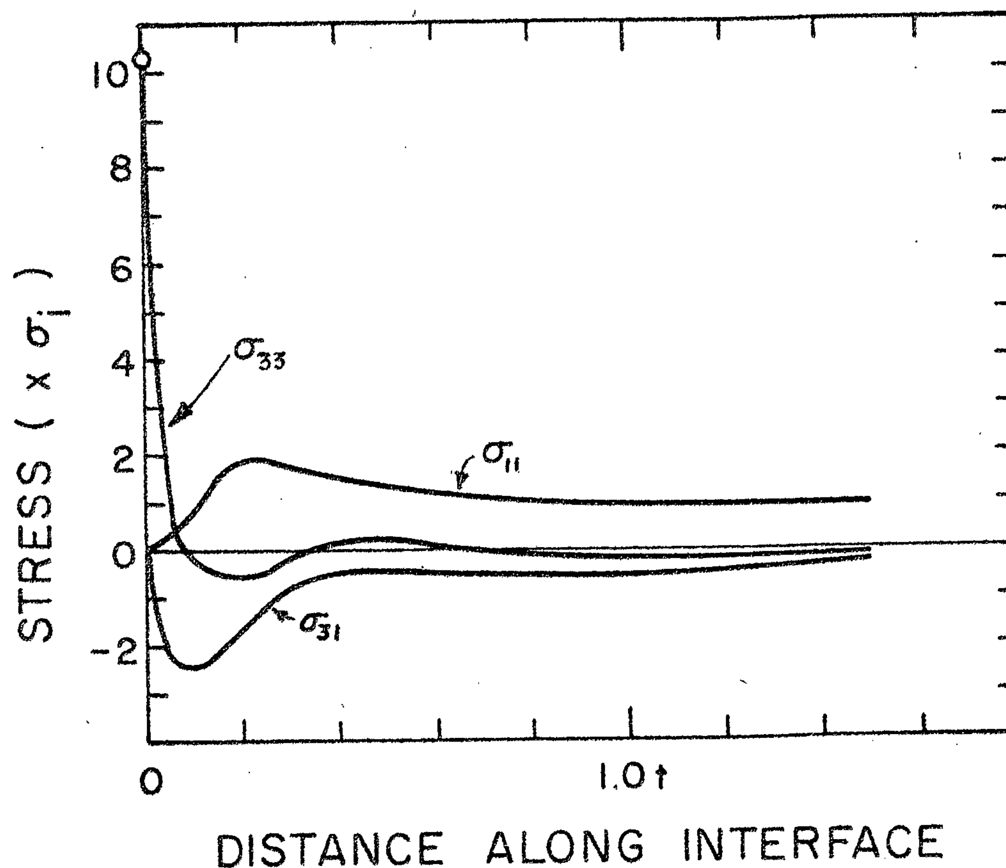

Figure 11. Interfacial stresses near the free edge of a semi-infinite film. After Doljack.[18]

stress until one gets within a distance of the order of the thickness to the edge. A large shear exists very close to the edge. In addition, a concentrated stress normal to the interface lies at the attached corner. We point out that there exist no non-zero stresses or stresses normal to the interface once one gets to a distance several times the thickness away from the edge. The presence of an extremely large normal force near the edge points out its relationship to failure at scratches or film edges. We will return to this phenomenon later.

Haruta and Spencer[24] have observed the spatial stress distribution by X-ray topography which is sensitive to the strain gradients, and qualitatively confirmed the rapid change near the film edge. A substantial decrease in strain was found after annealing.

To summarize then, we conclude by detailed calculations that as long as the substrate remains essentially rigid, and as long as we are not concerned with the stress distribution very close to the edges of the film, our simplified point of view which says only the components σ_{11} and σ_{22} are present, is indeed the correct one.

SECTION III - TECHNIQUES FOR STRESS MEASUREMENT

Introduction

Although the literature primarily quotes values for the stresses in films, it is actually strains that are measured. Two direct ways exist. First of all, a measure of the deformation of the substrate upon which the film has been deposited, or secondly, by diffraction techniques, a measurement of the elastic strain within the film or in some cases substrate. These two ways need not yield precisely the same values because of the distribution of forces across grain boundaries and within the grains of the fine grain deposit affect each technique differently.

A summary of the various methods used prior to 1970 for measuring the deformations has been well documented in the reviews by Scheuerman[10] Campbell,[7] and earlier by Hoffman.[4,5,25,26] We see no point for reproducing that information here. Many different techniques and their sensitivities were compared. In the last several years progress in measurement technique has been in several areas. First, the production of automated systems for measuring the stress on the routine basis on production samples.[26] The search for a technique of measurement of the stress on a localized scale on real structures has resulted in increased use of x-ray techniques. Holographic methods are not used commonly, perhaps because of some of the stringent vibrational requirements associated with that technique.

There has been recent progress in the refinement of the calculations used to relate the observed deflections of the stresses in the films. As the substrate temperature during deposition is perhaps the single most important parameter affecting the stress, its control or the correction for the various temperature factors in the measurement has also been of extreme importance, and progress has been made along these lines. We consider each of these areas in more detail.

Cantilever Plate Method

Perhaps the most common method for measuring the stress is the cantilever beam technique. Many have contributed to this type of measurement; it exists in a wide variety of detection schemes. Because good data is needed for further progress in understanding the origin of the internal stresses, and also because there is still a lack of appreciation for some of the subtleties in the experiment, we describe the cantilever method in detail; the information may be extrapolated to other geometries.

In the cantilever method the deflection of the free end of a thin plate is measured, or alternatively a force applied to the free end to restore the beam position to some fixed point. The other end of the beam is imagined to be clamped rigidly. This technique is often used because the deflection can be monitored continuously during deposition of the film and thus obtain information about the stress distribution. If the stress in the film is tension, as is commonly the case, then the film applies both a compression to the substrate and a bending moment. The stress is called tensile if the surface traction compresses the plate. This definition comes about because the plate applies a tensile stress to the thin film to prevent it from elastically relaxing. The resultant bending will be such that the film in tension finds itself on the concave side. The commonly used equation relating the deflection at the end of this cantilever beam to the force/unit width of the film is:

$$\delta = 3 \frac{(1-\nu_s)}{E_s} \frac{\ell^2}{h^2} F \qquad (8)$$

where ℓ is the length of the cantilever beam, E_s Young's modulus and ν_s Poisson's ratio for the substrate, and δ the deflection of the free end. It should be pointed out, although this is the presently accepted cantilever beam relationship, occasionaly the $1-\nu_s$ term, arising from the biaxial film stress, seems to be still neglected.

The concern, then, is how well this relationship actually describes the free end of the beam. The problem is one of properly describing the curvature in the transverse direction of the beam when it undergoes a large longitudinal curvature. This problem has been in the literature for a long time having been discussed as early as 1632 by Gallileo. St. Venant in 1864 presented the first mathematical formulation. The more recent treatments by Ashwell and Greenwood[27] and later by Bellow, et al.,[28] have given experimental justification for the treatment put forth by Lamb in 1891.

The results may be summarized as follows: Consider a plate of width b, length ℓ, and thickness h, bent to a longitudinal curva-

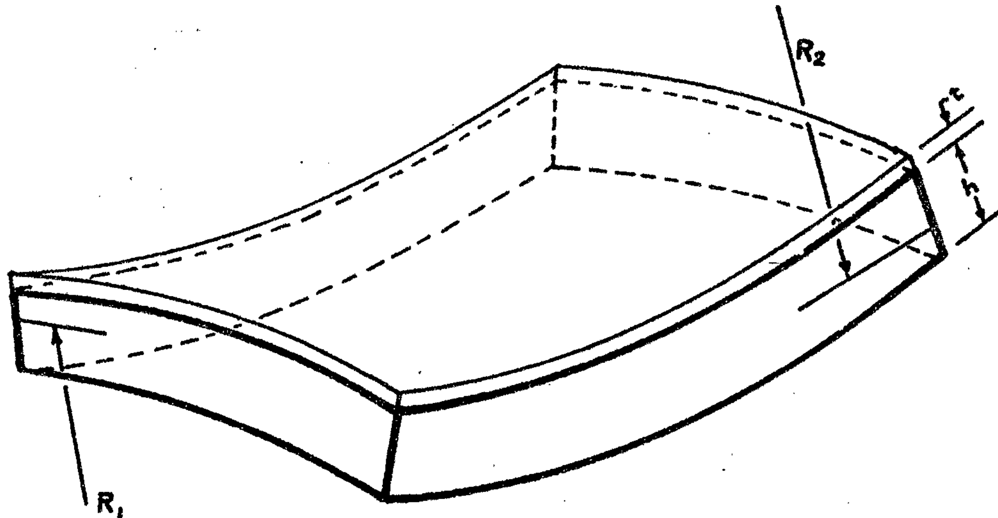

Figure 12. Anticlastic bending of a flat plate. From Bellow.[28]

ture 1/R by uniform moments applied to the ends. If the deformed shape is to be truly cylindrical, that is, the transverse strips are to remain straight, then moments equal to the moment in the longitudinal direction times Poisson's ratio are required along the long edges. Since such moments are not present the plate tends to assume a curvature ν/R in the transverse direction. This case is known as "anticlastic bending", and is illustrated in Fig. 12, the transverse distortion results in longitudinal membrane forces. As the curvature becomes larger the effect of these forces must be considered. It results in a stretching in the neutral plane and the Poisson effect eventually becomes cancelled leading to the case of cylindrical bending. The pertinent parameter in this problem is the ratio b^2/Rh. For values of this ratio from 0 to 1.6, the anticlastic case occurs. If the ratio is larger than 1000, then the surface can be considered cylindrical.[27] Under cylindrical conditions, the deflection of the end of the plate becomes smaller by the factor of $(1-\nu^2)$. As the transition from anticlastic to synclastic bending is a gradual one, the appropriate relationship must be known for the beam of our particular experiment. At present numerical calculations have compared favorably with experimental results for ratios up to 50.[28] By connecting the radius of curvature to the dimensions of the beam approximately through the rigidity relationship, one can write the ratio b^2/Rh in the form $2(b/\ell)^2\ \delta/h$. It is seen that for a beam whose length to width ratio is a reasonable 10, one may apply the anticlastic bending formula to the situation where the deflection is about 100 times the thickness of the beam itself. It appears that for practical purposes, unless one is dealing with a beam of rather square geometry, that the anticlastic formula will meet most practical purposes , and equation (1) or its equivalent for other geometry will suffice.

For the geometry of the cantilever beam the boundary conditions require that three edges be free while the fourth is clamped. Thus the deflection and slope of the plate as it emerges from the clamp are rigidly fixed. In practice, this seems to be a much more difficult condition to meet experimentally than is usually realized. The problem is often encountered when one uses a concentrated load at the end in order to determine Young's modulus for the substrate. Differences of as high as 20% are encountered between the apparent modulus values for the same beam measured by a cantilevered loading and a free beam loading. Rottmayer and Hoffman[29] pointed out that it is extremely important that the beam be gripped in the clamps such that no sliding would take place. Indeed, a rigid glueing is sometimes necessary. Resonance techniques are sometimes used to obtain values for E.[7,29]

Springer[30] has calculated the cantilever experimental arrangement on the basis of the linear bending theory of plates. The basic assumptions are that $\varepsilon_{33} = 0$, that is, there is no strain in the direction perpendicular to the plane. Secondly, plane sections remain plane upon bending which implies that no serious non-uniform stretching occurs and, thirdly, normal sections remain normal. This means that the transverse shear deformations are small. With these assumptions one proceeds as follows. The function for the shape of the plate is assumed, the stress distribution is given, and the total work done in forming the plate to a given shape is calculated and set equal to the strain energy stored in the plate for this configuration. Numerical calculations were necessary, and the result shows that the deflection calculated by the usual anticlastic relationship was 7% larger than the numerical calculation. This difference is probably due to the fact that the boundary conditions at the clamp is such that the beam may not have any cross curvature and the transition from this behavior to the anticlastic situation probably does not become apparent until about one beam width away from the clamp. The net result is to reduce the force necessary to bend the beam at the clamp and thus cause a greater deflection to appear at the end.

In practice it is probably not worthwhile to go through the effort of the numerical calculations and one should use the anticlastic relationship. It should be pointed out, however, that in careful experiments the error of about 7% in the bending equation may be comparable to other experimental errors. In order to compare numerical values for stress obtained amongst various laboratories one should make certain that the elastic equations used are described in the publication.

Detailed calculations of the deflection for another geometry have also been carried out. A free circular plate was first considered by Finegan and Hoffman[31] for the case of determining whether the stresses were anisotropic. As will become more obvious in the

next section, temperature control demands that any plate be attached to a thermal sink. Doljack and Hoffman[32] have solved the deflection equation for a cicular plate clamped along an inner circumference. One solves the problem by superposition of the deflection of the free plate and the deflection corresponding to the forces applied by the central clamp, under the condition that the intrinsic stress may be anisotropic. The plate itself wants to bend to the familiar elliptic paraboloid. The clamp at the inner radius applies those moments and shears to the plate that are necessary to change the deflection and give zero slope at the inner radius. The solutions can get rather complex because one must satisfy a fourth order differential equation, and enforcing the boundary conditions results in solving two sets of four simultaneous equations for four unknowns in each set. The resulting solutions are shown in Fig. 13, where it is seen that the centrally clamped circular substrate deforms in a manner very similar to the free circular substrate, with the zero deflection point moved out to the clamp.

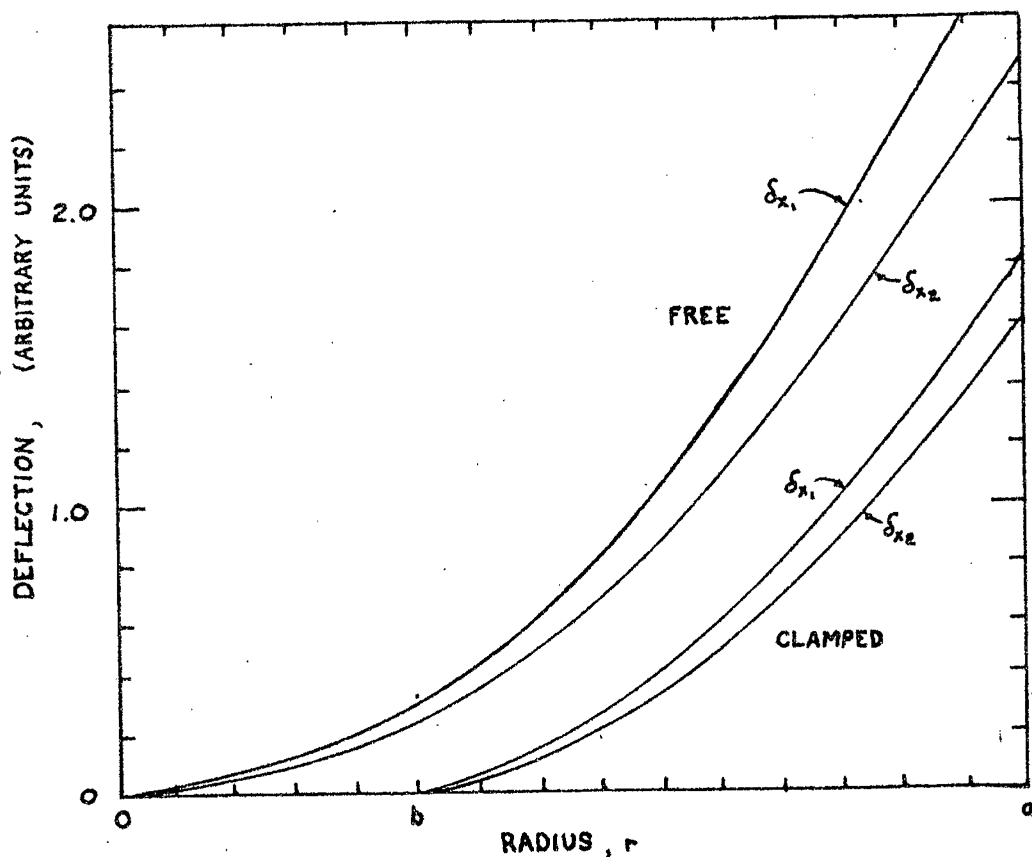

Figure 13. Anisotropic bending of a free and centrally clamped circular substrate. Doljack and Hoffman.[32]

It is also worthwhile noting the solution to the problem where the plate is clamped around its outer circumference. It is easy to show that under these conditions the clamp applies opposite bending moments that precisely cancel those applied by the surface traction. Thus, no deflection takes place. If a concentric hole is cut in the center of the plate, the plate will deflect and the solution will be the same as the problem previously solved with the roles of inner and outer radius interchanged. As one would expect, the overall bending produced by the same surface traction is less than obtained with the central clamp configuration.

The last configuration that is worth mentioning is the case of a free circular plate with a thin film deposited over the central circular area of the plate. The solution to this problem shows that as the outer diameter of the plate becomes very large, the bending of the plate in the region of the film does not decrease significantly. Although in practical problems the films deposited are seldom circular, the extrapolation of this statement is important for the case of many discreet devices on a single substrate.

The second area where a marked improvement has come about in the last few years is in the temperature stabilization of the substrate during deposition. Since the early work of Campbell and his co-workers in measuring the stresses in the early stages of deposition, it has been realized that both thermal and momentum effects are important. More recently, Kinosita[9] and his coworkers have shown how to make corrections to the deflections obtained during deposition. In their case for depositions of low stress metals on extremely thin mica substrates, the corrections were substantially larger than the observed deflections and in some cases of the opposite sign.

To illustrate the thermal contributions, let us take the cantilever beam of length ℓ, width b, and thickness h, and condense the film of density ρ or mass per atom m, at a rate R.

The momentum effect can be calculated by knowing the temperature T_m of the source, because that determines the velocity of the Maxwellian distribution of atoms as they leave. Assuming the arriving metal atoms do not rebound from the substrate, one can integrate the effect along the length of the beam and find the resultant moment. The result for the implied force and deflection from momentum consideration is equal to:[34]

$$\delta_m = 2.38 \frac{\ell^4 \rho}{E_s h^3} \left(\frac{kT_m}{m} \right)^{\frac{1}{2}} R \qquad (9)$$

where ρ is the denisty and m the atomic mass.

From the point of view of the experiment in which the deflection is measured as a function of the thickness of the film, this contribution would be a constant compression from the time the film starts to deposit until deposition is completed, assuming the rate of deposition is held constant, and the source temperature does not change.

Before we can say anything about the thermal effects, we have to establish the temperature history of the substrate. Maki and Kinosita[35], Yoda,[36,37] and Namba[38] have measured the temperature rise of 12 μm thick mica substrates during the deposition of silver films, by measuring the temperature with an iron-nickel thermocouple on the back side of the substrate. As indicated in Fig. 14, the shape of the curve is sensitively dependent upon the rate of deposition. Indeed, in films such as silver, the increase in the reflectivity of the thermal radiation may result in a decrease in the film temperature as the film becomes thicker. Note that the temperature rise may be quite large, perhaps 50° and saturate at thicknesses corresponding to the order of 1000 Å. Similar

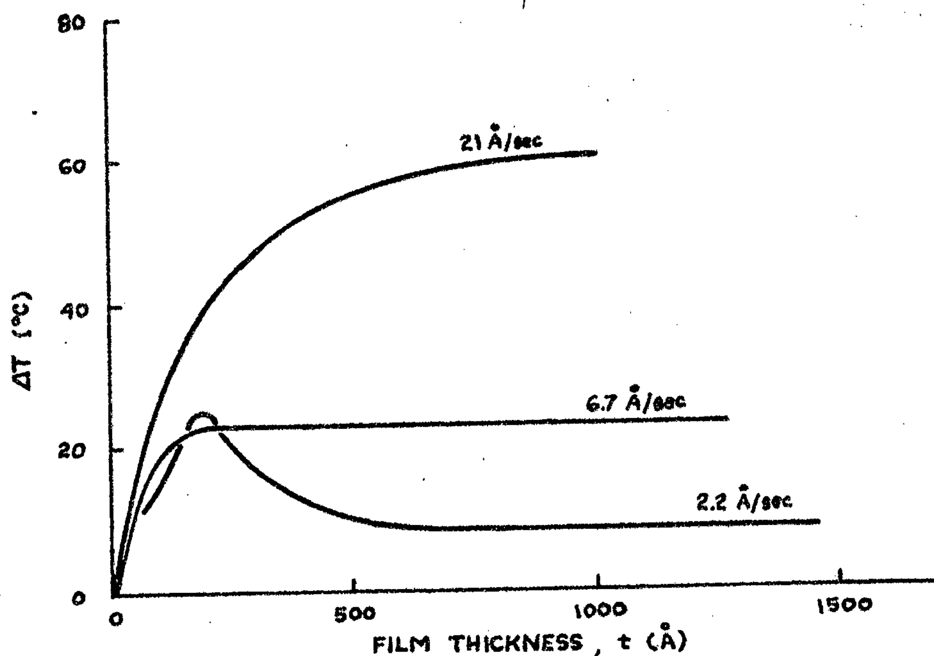

Figure 14. Temperature history during deposition of Ag on very thin, poorly conducting substrate. After Maki and Kinosita.[35]

experiments in our laboratory with extremely fine wire thermocouples bonded to the back side, show an increase in the temperature of the free end which is almost linear in the deposition thickness for deposition rates of the order of 25 Å per sec.

Normally, the cantilever beam is clamped at one end with a large thermal mass acting as a heat sink. At room temperature we assume the incident power must be conducted away from the substrate which produces the temperature gradient along the length. Assuming radiation negligible one may integrate the heat flow equations resulting in the temperature difference along the length

$$\Delta T_2 = \frac{P\,\ell^2}{2K\,h} \tag{10}$$

where P is the power per unit area incident on the substrate and K the thermal conductivity of the substrate. P includes the condensation energy as well as the energy radiated from the source and surroundings. For 'hot' sources the condensation energy is usually negligible, but the kinetic energy may be considerable in the case of high bias sputtering. For the evaporation geometry used by Springer,[30] P is 20 milliwatts per cm^2 resulting in a calculated temperature rise of 33° C. This estimate is perhaps 30% high compated to experimental evidence presumably resulting from the fact that steady state conditions are not reached and radiation losses are neglected.

Elastically, there can be several effects resulting from thermal expansion. First, the effect of differential thermal expansion between the film and substrate if the temperature of the specimen is uniform, but changed from T_{so}, the temperature of the substrate at the beginning of film deposition. Secondly, in a cantilever experiment, the temperature gradient along the length of the beam gives rise to a non-uniform bending, and thirdly, there is a temperature gradient normal to the film plane. All of these contribute, but the first two are interrelated.

Rottmayer,[39] Kinosita and Doljack have treated the first effect, under the model that the intrinsic stress is temperature independent and no stress relief takes place as the temperature is changed upon further deposition. A given layer deposits thermal stress-free, so there is a thermal stress gradient in the film from maximum at the interface to zero at the free film surface. The thermal strain may be calculated from the expansion coefficients α_f and α_s of the film and substrate. The result is, for a rigid substrate, equivalent stress or end deflection.

$$S_1 = \frac{E_f}{1-\nu_f}\,(\alpha_f-\alpha_s)(T_s-\langle T_s\rangle)$$

$$\delta_1 = \frac{3\ell^2\,E_f(1-\nu_s)}{E_s(1-\nu_f)}\,\frac{t}{h^2}\,(\alpha_f-\alpha_s)(T_s-\langle T_s\rangle) \tag{11}$$

where T_s is the final substrate temperature, assumed equal to the film temperature and $\langle T_s \rangle$ is the thickness averaged substrate temperature.

If the substrate temperature is linearly related to the thickness, then this net differential thermal expansion contribution vanishes when cooling to the average substrate temperature $\frac{T_{so}+T_s}{2}$ after the deposition is completed.

We consider now the case of a thermal gradient along the length of the plate. Elastically, this problem is not the same as the differential thermal expansion contribution that arises by changing the temperature of the substrate and the film by an amount ΔT_1. The reason for this is, of course, that the temperature gradient is not constant, giving rise to a non-uniform bending even though the average strain is still the same. The solution to this bending problem has been approximated by Alexander[34] giving rise to the smaller stress.

$$S_2 = \frac{1}{6} \frac{E_f}{1-\nu_f} (\alpha_f - \alpha_s) \Delta T_2 \qquad (12)$$

if the temperature difference ΔT_2 between the free end of the cantilever beam and the clamped end is established before the film is deposited. We see that this effect, too, may be eliminated entirely if the film and substrate have identical expansion coefficients.

These effects may have either an apparent tensile or compressive contribution but for the case where the α_f is larger than the α_s, the situation realized most often in practice, one finds that the contribution is an apparent compressive one. When related to the initial temperature T_{so} the third thermal effect arises from the temperature gradient through the thickness of the substrate. Although this contribution is extremely difficult to measure a worse case estimate of this gradient can be computed assuming that the incident power must be conducted from one side to the other. This gives rise to the equation $\Delta T_3 = P\,h/K$. Assuming the thermal expansion strains very linearly through the substrate the following expression is obtained for the effective force and deflection

$$F_3 = \frac{1}{6} \frac{E_s}{(1-\nu_s)} h\alpha_s \Delta T_3 \quad \delta_3 = \frac{1}{2} \frac{\ell^2}{h} \alpha_s \Delta T_3 \qquad (13)$$

For our experimental conditions the temperature gradient is 0.5 millidegree C. Table I summarizes these effects and compares them to the force/unit width for a high stress material, such as nickel at a thickness of 1000 Å. Unless the substrates are exceptionally flexible to obtain high sensitivity, we see that the momentum effect can be neglected for reasonable rates of deposition. Since the intrinsic stress is itself a function of the temperature of the

Table I

Comparison of Extraneous Effects in Cantilever Technique*

Effect	Temperature Change °C	Deflection cm	Force/ Unitwidth dynes/cm	Percent of 1000A Film
1000 Å Film	----	$2.5x10^{-2}$	10^5	
Substrate gravitational	----	$4x10^{-2}$	$1.6x10^5$	160
Film gravitational	----	$4x10^{-5}$	$1.6x10^2$	0.2
Momentum R=20Å/sec.	----	$5x10^{-5}$	$2x10^2$	0.2
Uniform temperature increase, Case 1	10	$3.7x10^{-4}$	$1.5x10^3$	1.5
Gradient along length - Case 2	30	$1.8x10^{-4}$	$7.5x10^2$	0.7
Gradient through thickness, Case 3	$5x10^{-4}$	$5x10^6$	20	0.02

*Calculated for a representative metallic substrate, 0.01 cm thick by 5 cm long and $\alpha_f - \alpha_s = 5 \times 10^{-6}$ °C^{-1}.

Stress in 1000 Å reference film is assumed to be 10^{10} dynes/cm^2.

substrate during deposition, it is then important to maintain the temperature as constant as possible. In terms of good substrate design one would then pick a substrate of high thermal conductivity and make the cantilever beam as short and thick as possible. The limitation to such an approach is usually the sensitivity of the deflection measurement.

Experimental Verification

Data for a cantilevered beam of the approximate dimensions used in our previous illustrations have been obtained by Springer and Hoffman.[40] For the case of a nickel substrate initially maintained at 32° C, the free end rose by 23° C. This temperature rise decreased as the temperature increased owing to the contribution of radiation losses. At approximately 150° C the temperature increase vanished and at temperatures above that, additional power had to be supplied in order that the substrate temperature did not fall during the deposition. A reproduction of the actual data for the case of a nickel film on a nickel substrate was shown.[40] A small compressional effect upon opening the shutter did not have a corresponding feature after the close of the shutter. Thus we conclude from the lack of a final transient that the compressional effect at the beginning of the film formation is a real phenomenon. For this experiment $\alpha_f - \alpha_s = 0$ and only a temperature gradient normal to the plane would produce an effect.

Even tighter temperature stabilization was achieved in the experiments of Doljack and Hoffman[32] with 2.4 cm dia., 0.015 cm thick (111) Si substrates. In part this was achieved by a shorter distance to the heat sink plus water cooling of the heat sink. With this geometry the temperature difference between the inner and outer radius was no more than 2° C over the temperature range

from 10° C to 200° C. The worst case increase in the average temperature was 10° C over this same temperature range. The average temperature increased linearly with film thickness up to about 100 Å and then remained constant for a deposition rate of 20 Å/sec. In these experiments, $\alpha_f > \alpha_s$ and differential thermal expansion gives a bending moment that decreases initially to some compressive value before coming constant when the substrate temperature reached its equilibrium value. Upon terminating the deposition, the force curve would rise toward a tensile value as the substrate temperature cooled to its original temperature. For the circumstance where the temperature increase took place up to roughly half the final thickness of the film the apparent tensile transient at the end of the deposition would be about 4 times the amount of the apparent compressive value. Maki and Kinosita[35] analyzed the more difficult experimental case of silver films on extremely thin mica substrates. Large transients with the thermal time constant took place after the close of the deposition. As was pointed out by the authors, the negative values of deflection are inexplicable. Furthermore, the decreasing deflection during the course of the deposition indicated that relaxation in the film was taking place. The silver films used in these experiments were probably responsible for the aging effects at extremely low temperatures.

In addition to the techniques treated in some detail in this section, we now list some of the techniques that have been used recently for deflection measurement. Many of them have been constructed for special measurements and it is suggested that the references be consulted for details. For *in situ* measurements during deposition, the force restoration techniques[40,41] and optical interferometers, in some cases using laser sources,[32,42,43,44] are the most widely used.

Holographic techniques, as proposed by Haines and Hildebrand[45] for macroscopic objects, were developed by Magill and Young.[46] To avoid the requirements of flatness and high reflectivity, Glang et al.[47] have surface profiled Si waters in orthogonal directions using a light-section microscope. The profile has also been determined by inversion of local radius of curvature data found by an optical lever method proposed by Axelrod and Levinstein.[48] Moire techniques have been useful in determining the principal stress direction in anisotropic films.[49]

Stress determinations using the bulge method were developed by Beams[50] in his studies of mechanical properties of metal films. Jaccodine and Schlegel[51] used this technique on an unsupported SiO_2 film by etching away the Si substrate, or by removing the oxide from one side and observing the resulting deflection. These concepts have been extended to a more local basis first, by Lane[52]

using a moat geometry and later by Lin and Pugacz-Muraszkiewicz[53] who have developed a technique to make deflection measurements on a microscale. Their technique uses standard photoresist methods to etch out a small bar-shaped sample and then free it from the substrate by etching with a second selective solution. If the film were initially under compression, upon being freed from the substrate it expands and deflects giving rise to considerable stress relief. The authors have analyzed the elastic problem in detail and have developed an expression relating the maximum displacement of the free oxide film, observed optically as indicated in Fig. 15, to the strain in terms of elliptic integrals of second kind. They have found that approximately 10% of the total stress remains

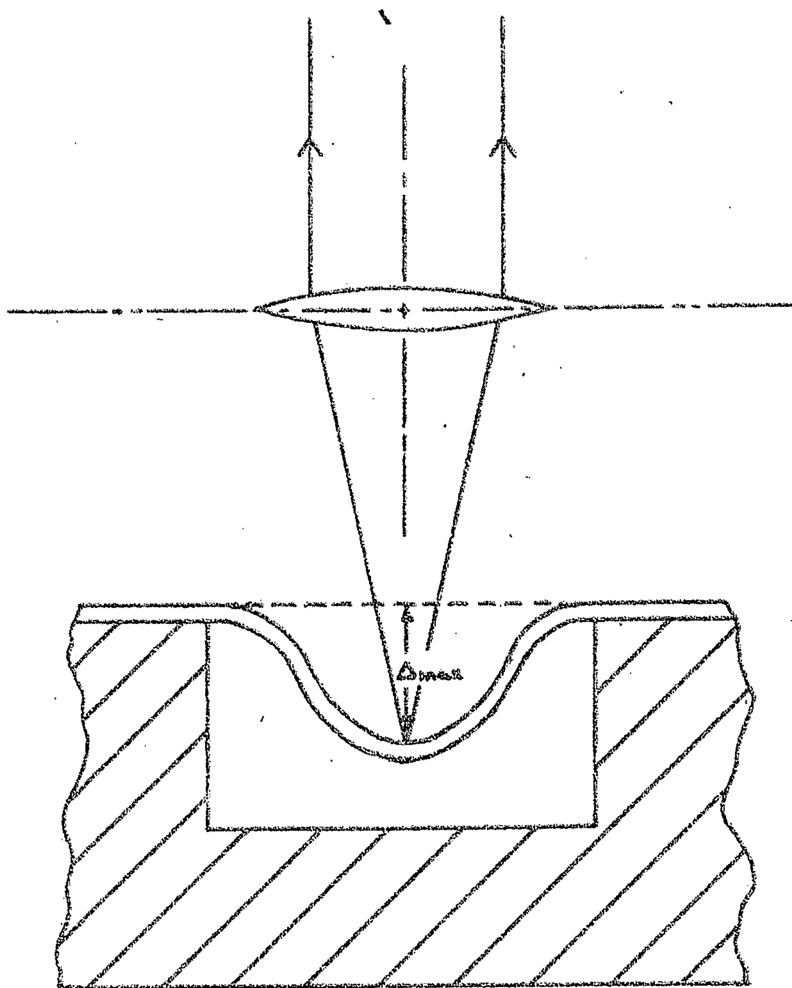

Figure 15. Moat technique for local stress measurement. Reference 53

in the deflected sample. With much less sensitivity this technique can also be used for films under initial tension by measuring the change in length of an undercut beam after it is released from the substrate. The technique has been applied to films under compression down to thicknesses of 250 Å for the case of SiO_2 on silicon and the results will be reported later.

A similar free-film technique is also reported by Wilmsen et al.[54] who considered the stability of the thermal SiO_2 film in relation to the thickness and width.

We summarize this section on the most commonly used technique for the quantitative measurement of stress in thin films by remarking that with sufficient care, the thermal difficulties may be overcome, the boundary conditions used in the calculations can be realized experimentally, and that interpretative data may be taken continuously during the deposition of a film in order to give information as to the stress distribution. The bending plate techniques have thus been very useful in studies dealing with the origin of the internal stresses and have even been used in automated systems on production samples through the use of fiber optics.[55] Microtechniques have led to localized stress distributions.

Thus we conclude with proper substrate design and choice of high thermal conductivity substrates, temperature effects may be reduced to the point where they are negligible for high stress deposits, even if thermal expansion coefficients are not matched. It is still true, however, that for measuring the stress in the early stages of growth or for materials which have a very low intrinsic stress, these problems have not been completely eliminated.

X-ray Methods

In order to follow the change in stresses through various processing steps, or in order to determine local changes in a stress as a function of position in the sample, x-ray techniques have been used. The more familiar one is to measure the lattice constant, usually with a diffractometer arrangement which determines the spacing between planes lying parallel to the planer surface. The strain in the film is most commonly measured but in a few cases the strain in the substrate has actually been used to infer the stress in the film. As usual, the stresses when calculated from the strain in the appropriate elastic constant, in this case the stress in the film plane in the simplest formulation is given by

$$\sigma_{11} = \frac{E_f}{2\nu_f}\left(\frac{a_o - a}{a_o}\right)_{33} \quad (14)$$

The elastic strain normal to the film is determined from the difference between the measured latticed constant of the film and the bulk lattice parameter.

Sufficient care must be taken in these measurements that changes in line shapes and shifts arising from stacking faults or homogeneous strains are not confused with the homogeneous component.

Recent progress in diffractometer methods follows. Zosi[56] measures the strain as the function of the angle from the normal to the film. Using only the position of the line centers, he finds a linear relation between the strain $\varepsilon_{\phi\psi}$ and sin 2ψ. The stress in the ϕ direction is then determined from

$$\frac{d(\varepsilon_{\phi\psi})}{d(\sin 2\psi)} = \left(\frac{\nu_f+1}{E_f}\right) \sigma_\phi \qquad (15)$$

for a biaxial stress. In this expression ψ is the polar angle and ϕ the azimuthal angle.

Bush and Read[57] simplify the expressions derived by Taylor[58] and also relate the film stress to normal and inclined diffraction angles upon specimen rotation. These treatments assumed no stress gradient normal to the film.

In order to directly measure the elastic strain, and thus eliminate the difficulty of using tabulated values for a_o the film may be detached from the substrate thus relieving the elastic strain and the lattice constant measured a second time. Kamins and Meieran[59] have successively used this technique for the stress in silicon films on sapphire substrates, through various processing treatments. The Nelson-Riley extrapolation function has been used to determine the lattice constant. Microbeam techniques coupled with scanning motion should allow the determination of the local elastic strain with a reasonable resolution. No such experiments seem to have been done.

Cullity[60] formulates the more general problem to consider the importance of line shapes. Borie[61,62] considers the effect of a linear variation of strain through the thickness. McDowell and Pilkington[63] derive a five-parameter nonlinear distribution from the line shapes which should be able to consider differences in structure at the free and substrate surface. In their results with gold films, immense elastic strains of 2.5% tension exponentially decaying within 100 Å of the glass substrate interface, slowly shift to compression in the body of the film and a large 2.5% compression near the free surface. The antisymmetric strain distributions in the thickness are a result of the symmetric diffrac-

tion peaks, but the authors offer no explanation for large strains and the lack of agreement with deflection experiments.

Within recent years an understanding of the topological x-ray contrast of imperfections in crystals has emerged through a study of both kinematical and dynamical effects.[64] As applied to stresses, contrast may be observed when a film deposited on a single crystal substrate provides a sufficient gradient to locally distort the crystal and give rise to intensity fluctuations. As previously described, Haruta and Spencer[24] used the technique to examine the stress distribution at the edge of a deposited film. Meieran and Blech[65,66] used Borrmann contrast to explain the diffraction contrast along interfaces. Schwuttke and Howard[67] regard the model as oversimplified and analyze the transmission geometry using the scanning oscillator technique following the treatment of Penning and Polder.[68] Dynamical effects and the lattice curvature resulting near the edges of an etched diffusion window give rise to the observed contrast. The strain gradient is a maximum at the window edge. Reference to Fig. 16 indicates that when the radius of curvature and the diffraction vector $\vec{g}$ are pointing in the same direction enhanced blackening is found on the film. If the substrate is found to be in tension then the film must be in compression, as illustrated in the figure. This technique provides good spatial resolution for the sign of the stress but quantitative information as to the magnitude is lacking. The authors also give illustrations of kinematical contrast at the boundaries where the adhesion is lost. Dynamical images obtained by either adjusting

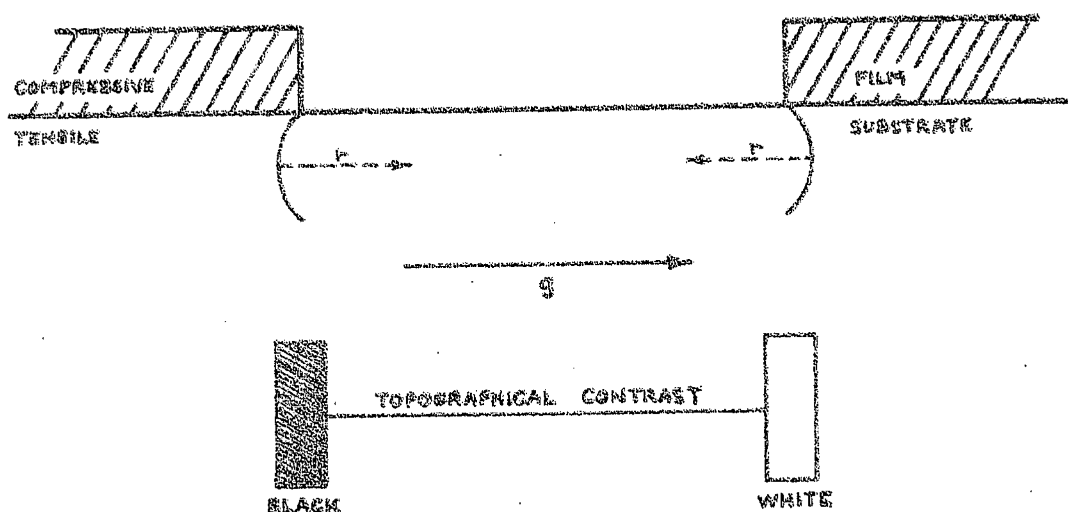

Figure 16. X-ray topological contrast according to Schwuttke and Howard.[67]

the substrate thickness or choosing the appropriate radiation give rise to unambiguous interpretation of the regions that have failed at the interface. It is worthwhile pointing out that localized adhesion losses were determined by this technique when the optical appearance of the film was mirror like and without any observable flaws. The authors also pointed out that these techniques make it possible to map the stress buildup in planar semiconductor devices. It is then possible to obtain information about the relative stress magnitude and the stress direction after each processing step, thus the stresses associated with the diffusion processes may be determined.

An x-ray double crystal arrangement in which the resultant topographs show the non-uniform variations of lattice orientation near the surface has been developed by Zeyfang[69] for thin silicon crystals bonded to glass. The origin of the strain may be inferred from the distinction between a uniformly distorted surface or one which has non-uniform distortions.

A modified scanning x-ray topographic arrangement has been developed by Rozgonyi and Ciesielka[70] which uses a feedback system to maintain a water orientation while the beam traverses the specimen. The radius of curvature may be determined with a spatial resolution of mm with simultaneous x-ray topographs. Stresses in both very thin films (∿ 100 Å) and substrate are calculated; as well as effects of diffusion and ion implantation.

Because of the availability of x-ray topographical techniques for semiconductor defect studies, their increased application to stress systems caused by deposited films, diffusion, or implantation is expected. Both lattice parameter and topological methods are non destructive, have good spatial resolution and sensitivity, but are not convenient nor rapid enough to be used during deposition.

Other Techniques

A new technique by EerNisse[71,72] has been developed for simultaneous measurement of stress and mass change. This double quartz crystal resonator technique uses AT cut and BT cut crystals such that the sum of the frequency shifts is proportional to the mass change and the difference in the frequency shifts is proportional to the change in the thin film stress. The sensitivity is quoted at 125 dyne/cm for a 10 Hz frequency shift. The technique is suited best for stress studies when the mass change is quite small, and has been used in connection with implantation studies on silicon samples.

Any physical property may be used to determine the stress, and examples are beginning to appear. Note that this is the inverse of the usual case in which the 'unusual' properties of a film are being explained in terms of the stress, and represents a more sophisticated point of view. Oel and Frechette[22] have done this for macroscopic glass discs using birefringence to measure the strain. Reinhart and Logan[73] calculated the phase difference and elastic constants from the crystal piezo-optical tensor coefficients, and compare with data to determine the interface stress of thick epitaxial layer structures. Fig. 17 gives the stress distribution near the interface for $Al_{0.1}Ga_{0.9}As$ on (111) Ga As.

An increased use of such 'indirect' measures of the strain is anticipated.

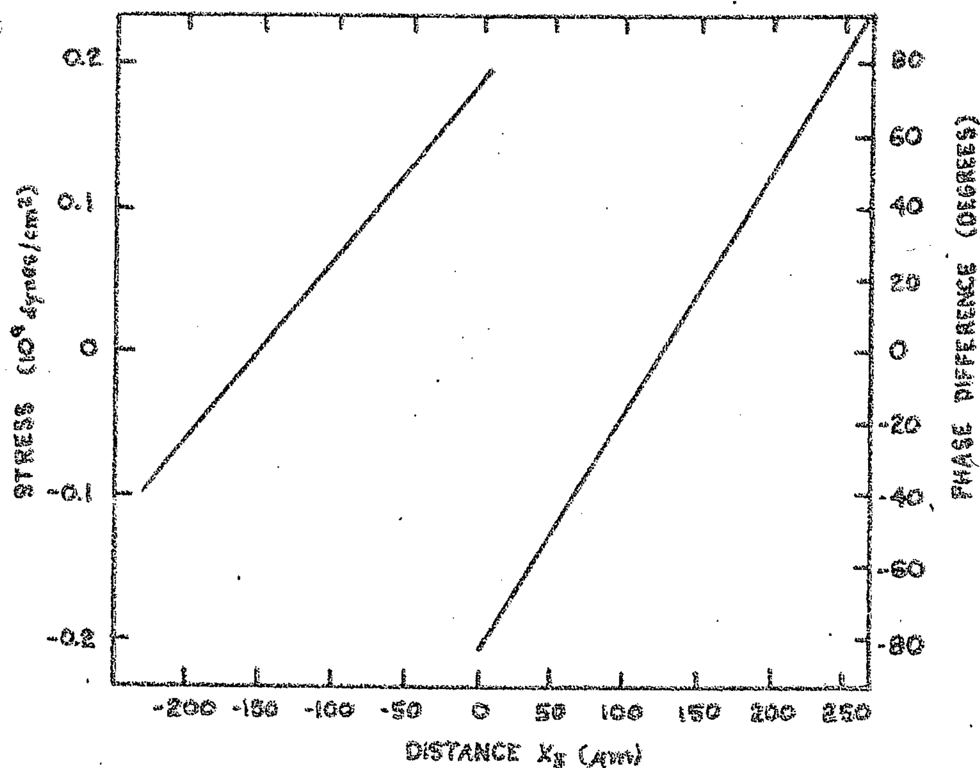

Figure 17. Stress distribution from optical birefringence measurements of Reinhart and Logan[73] in GaAs.

SECTION IV. THERMAL STRESSES IN THIN FILMS

Introduction

The techniques for measurements that we have discussed in the preceeding sections have allowed the determination of a strain and the calculation of an associated stress. We now turn to the questions of the origin and the various mechanisms that can contribute to these strains. As a matter of definition the total stress in the film is regarded as being made up of two possible contributions. These are defined as the differential thermal expansion stress whose origin is understood, and whose value is generally amienable to calculation, and, the intrinsic stress which is the manifestation of all other contributions. We may write $\sigma_T = \sigma_{DTE} + \sigma_i$, where the intrinsic stress, σ_i, may be composed of several terms.[1] Clearly, σ_T is measured and a property responds to the total stress. The contributions from either term may be tension or compression, with the resultant total stress in the film being determined by the relative magnitudes.

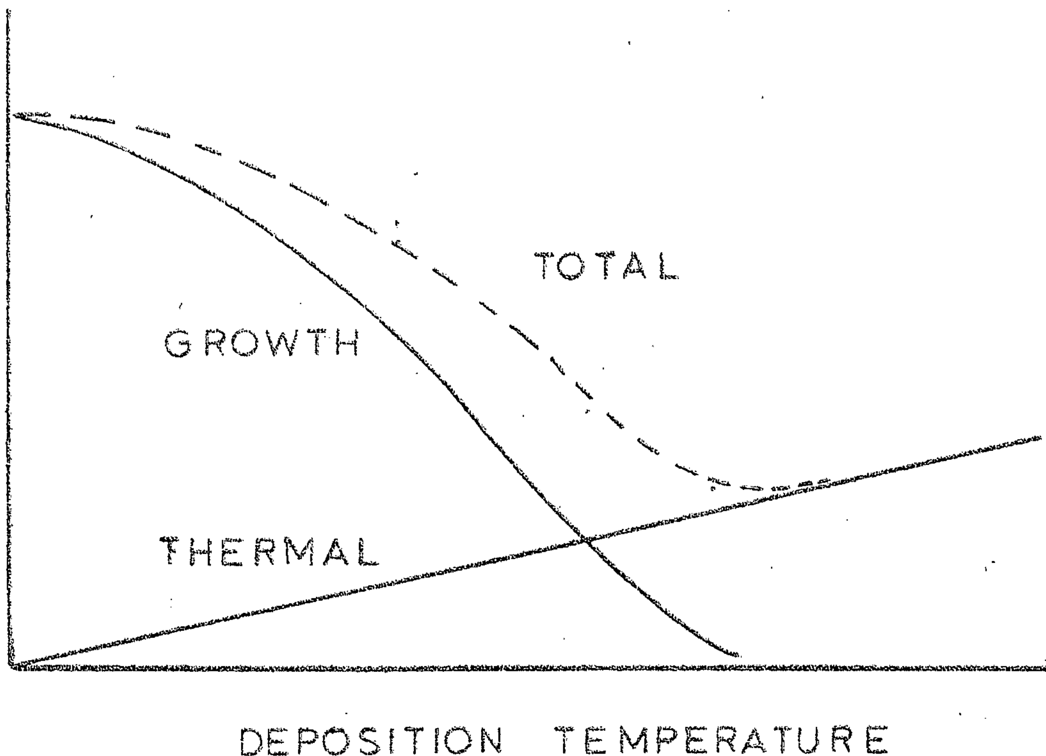

Figure 18. Thermal and intrinsic stress contributions.

In Fig. 18, we consider in an idealized way the case of a film deposited on a substrate at temperature T_s and cooled to the final temperature T_m. If the thermal expansion coefficient α_f of the film is larger than the expansion coefficient of the substrate α_s then the contribution to the stress from differential thermal expansion increases linearly as the substrate temperature increases. On the other hand, the intrinsic stress is often a decreasing function of the temperature, so that the total stress in the film may, in fact, have a minimum at some intermediate temperature.

Even today the literature far too commonly considers differential expansion as the only contribution to the stress. For the higher melting point metals, for example, intrinsic stresses are quite large up to substrate deposition temperatures of several hundred degrees C. In other systems the diffusion of impurities into or out of the film at elevated temperatures give rise to substantial stress effects. Even in the case of thermally grown SiO_2 on Si at high temperatures, the intrinsic stresses have an important role.

On the basis of our earlier sections we see that the fundamental origin of all of the strains in films lies in the constraint that the film is being tightly bonded to the substrate and after this bonding has taken place there is a subsequent volume change in the film (or strictly a planar distortion). Thus, in addition to the same assumptions made in solving the elastic problem, we must evaluate the strain itself. Normally this is simplified by assuming the substrate is rigid and that neither contraction nor bending takes place in the film substrate. Under this assumption the change in lengths of the substrate resulting from the stresses on it is negligible, but if the film and substrate were of comparable thickness, then both of these relaxation effects must be taken into account.

Thermal Expansion Stress

Normally, the thermal expansion strain is considered to be isotropic. In general, the coefficient of thermal expansion relate the strain tensor to a small uniform temperature change. Thus, the thermal expansion tensor is symmetrical since the strain tensor is.[12] It is worth noting that since the thermal expansion of a crystal must possess the symmetry of the crystal, it cannot destroy any symmetry elements and this is why the class of a crystal does not depend on the temperature. The thermal expansion tensor may be referred to principal axes and thus reduce the number of coefficients to 3. For most substances the principal thermal expansion coefficients are all positive. But in a few crystals,

for intance calcite, or silver iodide, some coefficients are negative.

We may write the nine thermal strain components in terms of the thermal expansion tensor.

$$\epsilon_{ij} = \alpha_{ij} \, \Delta T \qquad (16)$$

where the identical subscripts refer to the normal components and the mixed indices to the shears. The thermal expansion tensor is often reduced to a column matrix to be consistently used with the six single index strains ϵ_i.

$$\epsilon_i = \alpha_i \, \Delta T. \qquad (17)$$

If we consider the restrictions of crystal symmetry,[13] only in the triclinic and monoclinic systems are the shear coefficients other than zero. The orthorhombic system has three independent normal expansion coefficients, the tetragonal, trigonal, and hexagonal systems have two, and the cubic system has an isotropic thermal expansion. We must point out however, that even though the thermal expansion may be isotropic, because the elastic constants are fourth rank tensor properties, anisotropic stresses will be obtained even in a cubic crystal. Only if the sample may be considered to be elastically isotropic, that is in practice a polycrystalline sample with random grains, will the resultant thermal expansion stresses be isotropic. Once the thermal strains are determined, the stresses are calculated from the appropriate elastic constants. The equation

$$\sigma_{DTE} = \frac{E_f}{1-\nu_f} \epsilon_{11} = \frac{E_f}{1-\nu_f} (\alpha_f - \alpha_s)(T_s - T_m) \qquad (18)$$

is proper for the rigid isotropic case and takes account of the biaxial stress generated by the linear strain $\epsilon_{11} = \epsilon_{22}$.

The sign is such that the tensile stress is positive. Obvious extensions are needed when the temperature range considered is so wide that the α's are no longer constant. Vook and Witt[14,74] carried out calculations of the strain normal to the plane of the film for arbitrary orientations of cubic crystals. In these calculations which were also extended to include the strain energy it was assumed that the shear strains in the film were zero. For copper and silver, the metals considered, the strain energies were found to be in the same relative ranking as Young's modulus. Vook and Witt point out that the observed line shifts in an x-ray diffractometer experiment when the temperature is changed correspond directly to the calculated thermal strain, even though other

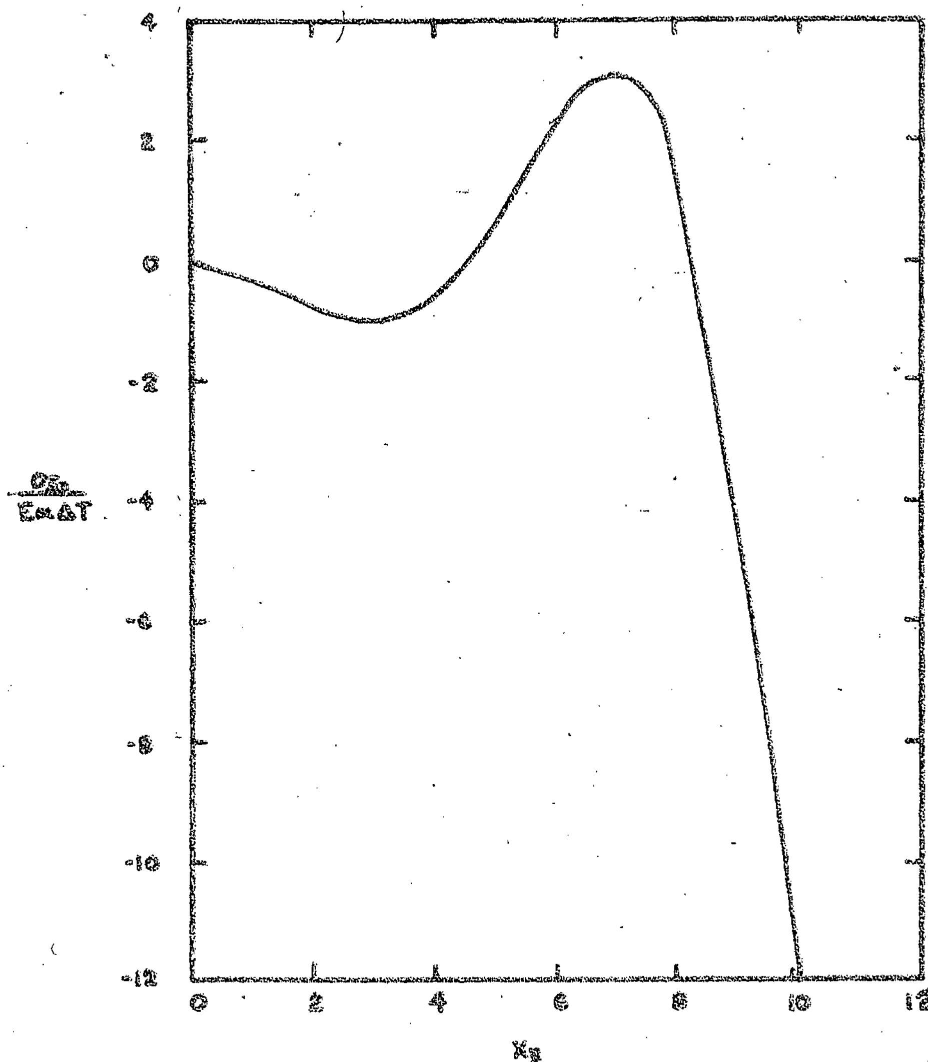

Figure 19. Thermally generated normal stress at a free edge as a function of distance from the free surface. After Aleck.[23] Coordinate $x_3 = 10$ corresponds to the interface.

contributions to the line positions as a result of faulting may be present.

To this point we have considered the specimens to be semi-infinite in size and edge effects have not been important. Aleck[23] has converted the thermal stress problem in a rectangular plate clamped along an edge to one of boundary stress conditions.

His two dimensional solutions indicate there are large shear stresses present in the film within about two film thicknesses of the edge, and a stress normal to the plane of the film concentrated at the intersection of the edge of the film with the film substrate interface. The distributions along the interface (clamped edge) are qualitatively similar to the data in Fig. 11 if normalized to the one-dimensional thermal stress $E\,\Delta\alpha\,\Delta T$. The large variation of the normal stress σ_{33} as a function of the distance from the free surface at the edge of the film is given in Fig. 19.

Zeyfang[75] has extended Aleck's approximate solution to plates of arbitrary lengths, rather than the semi-infinite plate used by Aleck. He also gives detailed stress, strain and displacement distributions for plates with length to thickness ratios of 2, 5, and 15. Compared to the semi-infinite case where there are edge effects only, when the length of the film becomes short enough, nonuniform stress distributions are found throughout the volume of the film. The maximum stress in the plane of the film decreases as the sample length decreases and actually reverses sign on the free surface of the film for samples that are only twice as long as their thickness. The maximum shear stress decreases with increasing plate lengths and the stress normal to the plane in the center of the interface increases with decreasing plate length. Zeyfang points out that for plates whose length to thickness ratio is greater than 15, it is possible to think of the distributions as being composed of a uniform part for the central part of the sample and edge terms, but such a treatment is not valid for shorter samples. The shape of a half film under the exaggerated thermal expansion condition is shown in Fig. 20. Because of the singularity of σ_{33} in linear elasticity theory at the interface edge, a cylindrical cavity was cut out and the displacements approximated by surface displacements. For such short samples it follows that the upper surface no longer remains plane under a thermal expansion strain.

In carrying out the calculations of thermal expansion contributions the questions arises as to the values of the thermal expansion coefficient to be used. There seems to be no evidence for abnormal expansion coefficients in deposited films. There are cases where the total stress effects do not seem to coincide with calculations of the thermal contributions, but these are attributed to irreversible intrinsic stress changes in the film upon heating. Hence, tabulated values of the expansion coefficient seem quite suitable in practice. Feder and Light[76] have reported an apparatus for directly measuring the differential thermal expansion between a film deposited on the substrate by observing the optical fringe shifts corresponding to bending the sampe. For the case Ge/Ga As film couple the difference between the thermal

expansion coefficients is demonstrated to be less than 1 part in 10^8.

One of the goals of the calculation of thermal stresses is the prediction or explanation of properties from data on bulk, strain-free samples. Schlötterer[77] determined the resistivity change in epitaxial Si on spinel in terms of the piezo-resistance coefficients for isotropic thermal stress. A second example is the anisotropic Hall mobility found in silicon on sapphire films by Hughes and Thorsen.[78,79] After calculating the thermal expansion stresses arising from the anisotropic thermal contraction

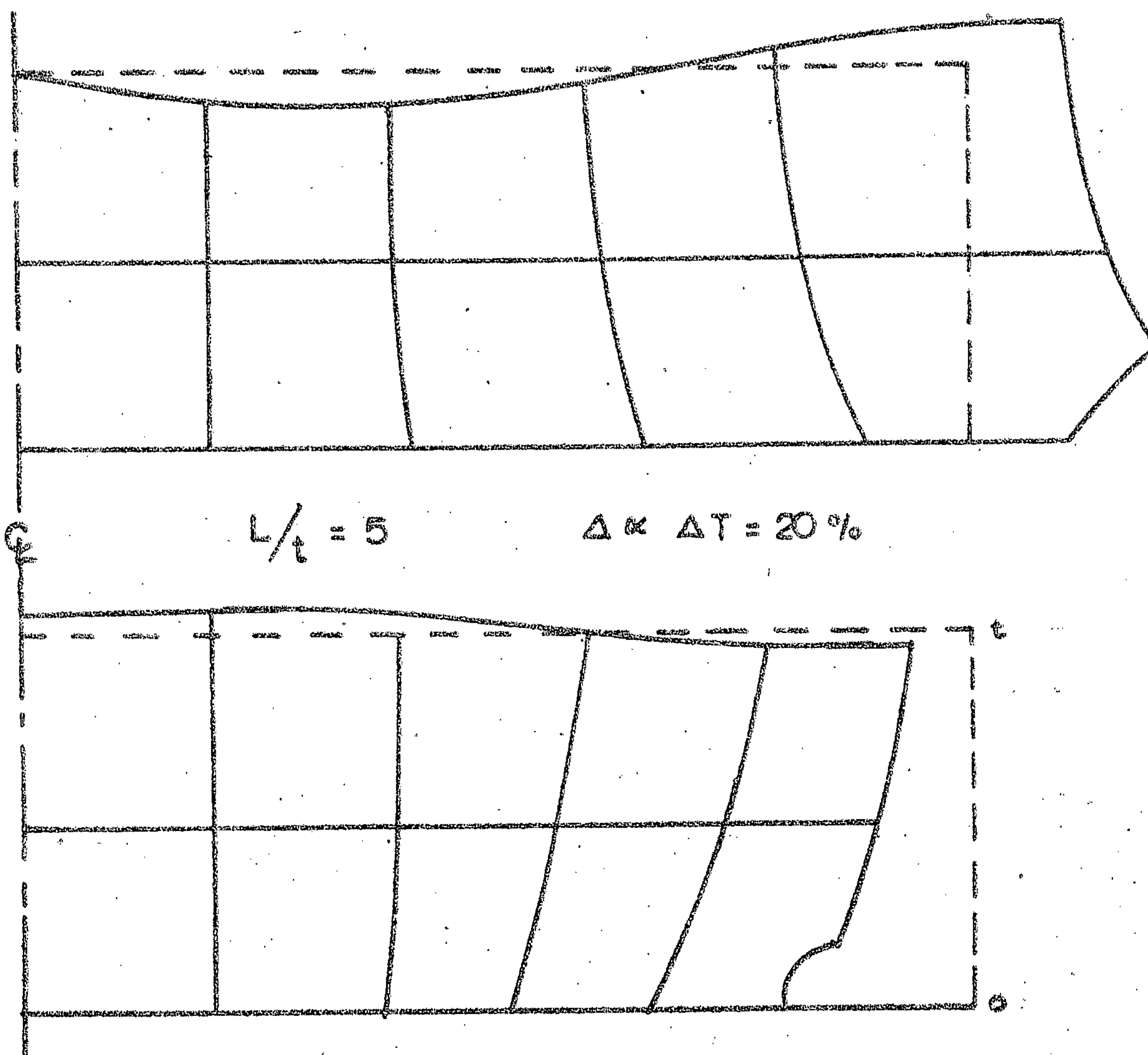

Figure 20. Thermal expansion distortions of short films according to Zeyfang.[75]

of Al_2O_3 in cooling from the deposition temperature, they also use the piezo-resistance effect to relate to the Hall mobility. The approximate 10% anisotropy of the Hall mobility in two orthogonal directions seems adequately described in terms of thermal strains. Hughes[80] carried out detailed calculations of the effect of stress on resistivity for general orientations in several crystal systems.

Thus it appears as though both isotropic and anisotropic thermal expansion strains, and their effect on transport properties are amenable to calculation.

SECTION IV. ORIGINS OF THE INTRINSIC STRESSES

The review articles by Hoffman,[4,5,6] Campbell[6,7] Buckel,[8] and Kinosita,[10] all have the goal of trying to assimilate the massive experimental literature on measurements of the stress and attempting to interpret them in a few simple concepts. In addition to the thermal stress, Buckel lists six other processes which may produce stress in the following way.

1. Incorporation of atoms, for example, residual gases or chemical reactions.

2. Differences of the lattice spacing of monocrystal and substrates and the film during epitaxial growth.

3. Variation of the interatomic spacing with crystal size.

4. Recrystallization processes.

5. Microscopic voids and special arrangements of dislocations.

6. Phase transformations.

In addition, all of these processes may occur both during condensation and growth of the film and under annealing conditions afterwards. A search of the literature also indicates that most of these models have been developed to explain the stress in metallic films, pure metals or some simple alloys. Especially with nonmetallic films, where the stoichiometry and the structure is still far from being well established, the understanding of the origin of the stress is now unsatisfactory. For these reasons we review the models for the intrinsic stress very briefly, calling attention to those cases where there is some confirmation in the literature for non-metallic films. More importantly, the discussion may give a physical basis for the application of these concepts to non-metallic systems. Many of the models find it

relatively easy to explain shrinkages and hence, tensile stresses in the film, but can explain compressive behavior only with difficulty.

Several different kinds of processes may operate in the first classification. Nakajama and Kinosita[81] have measured the stress in silver films deposited at 10^{-3} and 10^{-6} Pascal and find the following behavior. The dependence upon the thickness is not greatly influenced by the deposition parameters before the film becomes continuous. The residual gas pressure during the deposition has no appreciable influence on the stress behavior. However, after the deposition the stress will remain at its constant tensile value if the sample is kept in a vacuum of 10^{-6} Pascal but if kept in a 10^{-3} Pascal surroundings, a compressive relaxation to a smaller value of tension in the film is found. Furthermore, this compressive contribution will recover with a time constant of the order of hours if the pressure in the system is reduced to 10^{-6} Pascal. The authors suggest the reason is the absorption of residual gas in the film, and the stress effects correlate with changes in the electrical resistivity.

Actually, the presence of residual gas, oxygen and water vapor in particular, has long been suspected in the case of those metallic films showing compression when deposited in poor vacuum, or when annealed in air after deposition. A more direct quantitative confirmation of the effect of gas incorporated in the film during the deposition process has been forthcoming in the work with bias sputtering which we shall treat in some detail in a later section. Ion implantation which clearly gives rise to dilation also falls in this category.

Because of their technological importance, the growth stresses in thermal and anodic oxide films must be included. A recent review by Stringer[82] considers the stress generation and relief in grown oxide films on metals. The sign of the stress in the oxide layer may be predicted by the ratio of the volume per metal ion in the oxide to the volume of metal atom in the metal or the Pilling-Bedworth ratio. Most grown oxide layers are compressive but MgO is correctly predicted to be tensile although actual stresses are much less than calculated by this ratio. These differences may arise from ion motion, particular anisotropic growths, or, perhaps more likely, plastic flow taking place during the oxidation process. A second mechanism includes the oxygen migration down grain boundaries in the metal oxide in order to react with metal ions diffusing through the bulk. This mechanism, illustrated in Fig. 21, also leads to a compressive growth stress in the oxide according to Rhines and Wolf.[83] The similar impurity migration down grain boundaries has been suggested as the origin of the compressive stress in metallic films.[32] A

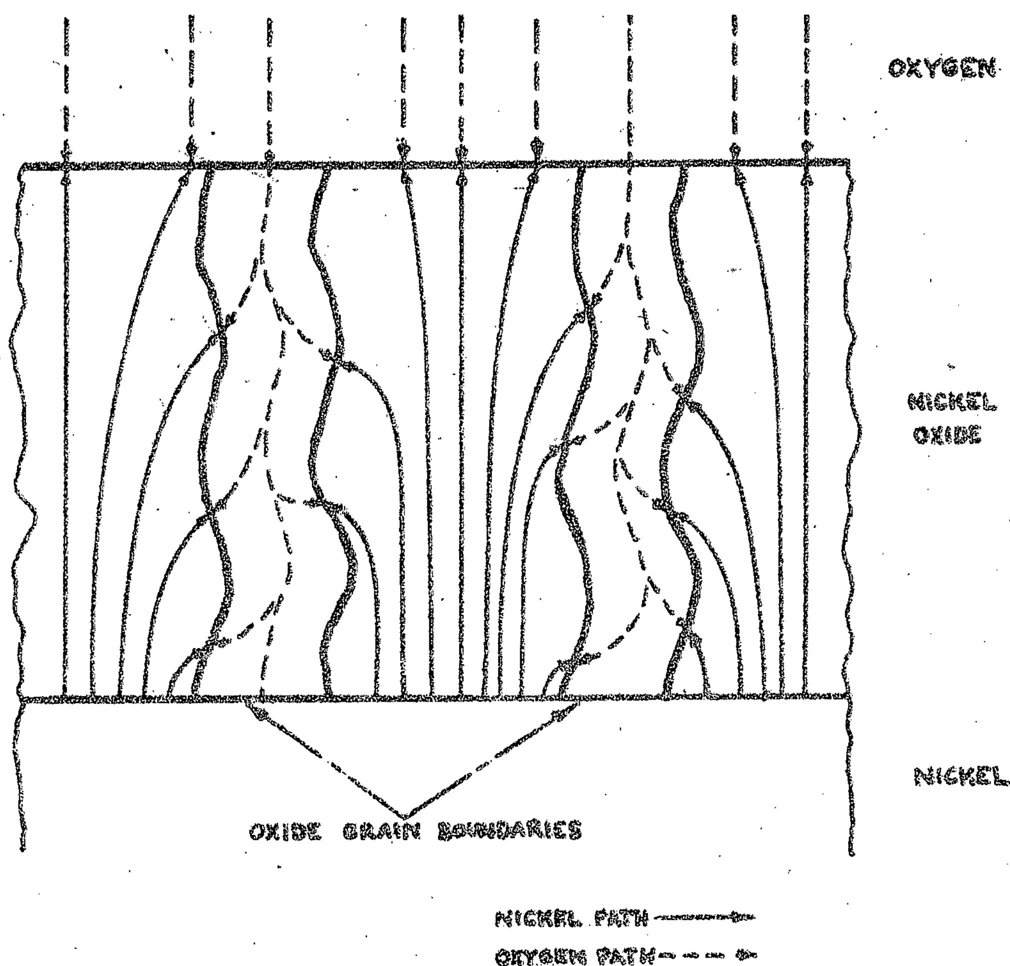

Figure 21. Schematic diagram of diffusion paths. Following Rhines and Wolf[83] and Stringer.[82]

similar situation is found in the growth of anodic oxide films, which have recently been reviewed by Dell'Oca et al.,[84] following earlier articles by Young[85] and Vermilyea.[86] The growth of intermetallic phases following diffusion has been confirmed as a stress mechanism.[137]

One of the best documented origins of internal stress occurs during epitaxial growth as a result of the efforts of Van der Merwe[87,88,89] Matthews,[90,91] Jesser and Kuhlmann-Wilsdorf,[92,93] Honjo[94] and others. An interfacial energy,[92,93] is calculated which depends on the differences of the lattice spacings of the substrate and film, as well as the elastic constants of each material. For small mismatches or thin films, the total energy

in the system will be minimum if the film developes a uniform elastic strain. However, if the film becomes thicker or if the mismatch is more severe, the energy of the system may be lowered by the creation of an array of interfacial dislocations which may relieve a large fraction of the strain in the film. A total or partial elimination of misfit dislocations may take place as schematically indicated in Fig. 22, where the energy gain is ΔE and the critical misfit is seen. It is worth noting that forces normal to the interface contribute only about 10% of the interfacial energy. Recently the misfit dislocation energy is calculated[88] from a periodic interfacial potential which is a generalization of a Pierls-Nabarro model rather than the older pair-wise or elastic models.

Jesser and Kuhlmann-Wilsdorf[92,93] have shown that a similar formulation holds for films in the isolated island stage of growth. The interfacial dislocation mechanism for the origin of intrinsic stress is attractive because it may be formulated quantitatively and compared with experiment. As a general mechanism, however, it must be criticized on two grounds. First, the obvious one that it is not easy to see how such a mechanism would operate for growth of polycrystalline films and, secondly, in this model the strain is localized and decays exponentially from the interface and thus does not project the constant stress often experimentally found. Nevertheless, data for 50 Å polycrystalline alkali halide films on glass seem to follow this model.[95]

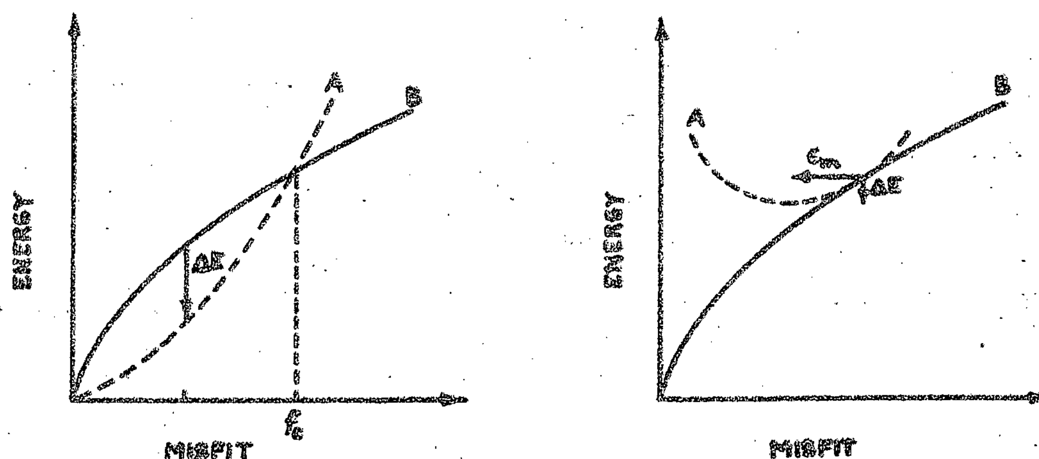

Figure 22. Energy gain ΔE arising from total or partial elimination of interfacial dislocations. Curve A is the homogeneous elastic strain energy, and B the misfit interfacial energy. After Van der Merwe.[87]

A stress model for heteroepitaxial films combining thermal stress and assuming the film lattice constant is constrained to match the substrate has been developed by Besser et al.,[96]

They have examined many CVD magnetic oxides and developed a physical model in which the film stress is entirely determined by uniform misfit at room temperature independent of the deposition temperature up to a critical value and entirely by thermal expansion for larger misfits. This idealized model works well when the thermal expansion coefficients of film and substrate are nearly the same. It takes account of the thermal expansion in region I by using the room temperature lattice constants but assumes the complete relaxation of the mismatch stress in region II.

Fig. 23 indicates these two regions, where

$$\sigma_I = \frac{E_f}{1-\nu_f}\,\frac{(a_s-a_f)}{d_f} \qquad \text{and} \qquad \sigma_{II} = \frac{E_f}{1-\nu_f}\,(\alpha_f-\alpha_s)\Delta T \quad .$$

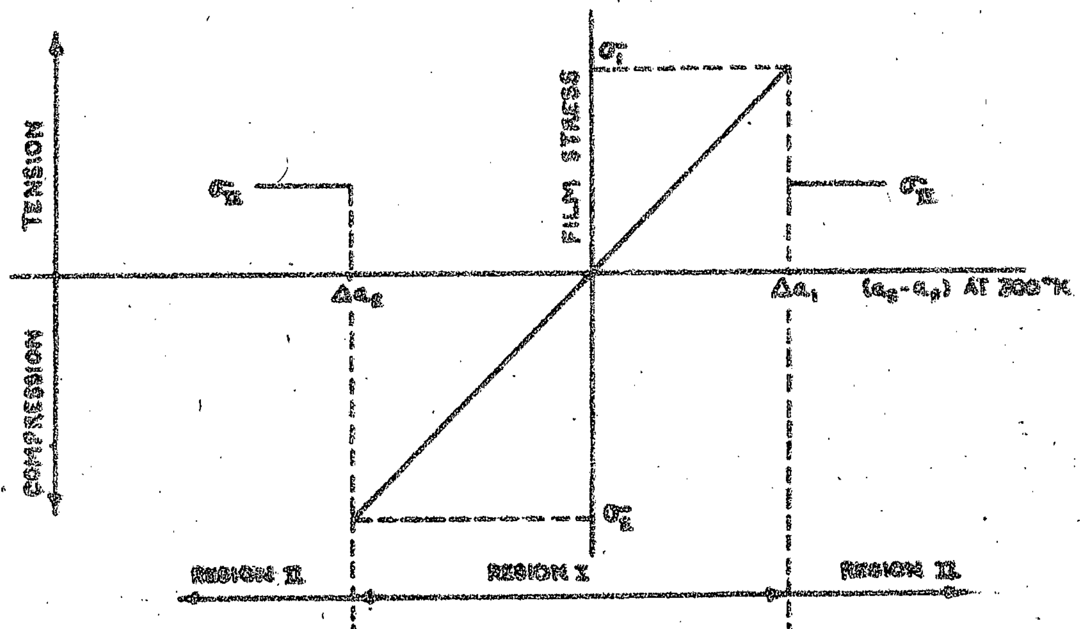

Figure 23. Epitaxial misfit-thermal strain model of Besser et al.[96]

Carruthers[97] proposed a similar model including the effects of plastic deformation occuring at strains larger than 0.005. He fits the thermally-activated glide relation derived by Matthews et al.,[91] in which the misfit strain is the driving force to the data of Besser et al. Carruthers' expression for the planar strain is

$$\epsilon_{11} = \left(\frac{a_s^{T_m} - a_f^{T_m}}{a_f^{T_m}}\right)(1-\xi) + (\alpha_f - \alpha_s)(T_s - T_m) \qquad (12)$$

where

$$\xi = \left|\frac{a_f' - a_s}{a_f - a_s}\right| \Bigg|_{T=T_s}$$

ξ is the fractional strain recovery and is a measure of the actual strained film lattice constant a_f' and the lattice parameter of the film material a_f both evaluated at the deposition temperature T_s. Braginski et al.,[98] gives additional data for the magnetic oxides.

In the third category, one finds a number of experiments relating the lattice constant with the crystallite size and interpreting the results in terms of a surface energy. Cabrera[99] formulated the thermodynamics following the classical paper by Herring.[100] Linford and Mitchell[101] introduce the concept of interplanar potentials which relate the surface work to macroscopic parameters of elastic constants and thermal expansion coefficients. Wasserman and Vermaak[102] give recent data and references for the surface stress as observed by electron diffraction. The surface energy provides a recognized contribution generally giving a compressive stress in the isolated island stage of growth,[99] however, unless the growth of a deposit can be formulated in terms of a continual nucleation and growth framework it is difficult to see how this category can contribute to the stresses in thick films. It remains then a difficult experimental area because of the vacuum environment, but in need of future work.

The surface stresses in Ge, InSb and GaSb have been measured using the bending of thin samples by Taloni and Haneman.[43] The effects of surface stress as correlated with bending plate measurements have been discussed by Hoffman.

Classification 4, recrystallization processes, contains a number of different models that differ in their details. Klok-

holm and Berry,[105] suggest that the stresses are generated "by the annealing and constrained skrinkage of disordered material buried behind the advancing surface of the growing film." The magnitude of the stress is determined in this model by the amount of disorder at the time the atoms become constrained and the subsequent annealing during condensation process. The temperature dependence of the intrinsic stress is determined by the kinetics and it is held that no stress would be found in films deposited at extremely low temperature substrates, and at substrate temperatures during deposition higher than about 1/4 of the melting temperature. This form is approximately followed for metals. In this model, films deposited on cold substrates would have no stress since the atomic rearrangement is no longer possible.

The helium temperature experiments of Buckel[8] indicate that simple metals growing in the normal crystalline phase, even though they have very small crystals and have a high degree of disorder, do develop large stresses when deposited at these very low temperatures. It is often stated that amorphous films have low stress. Gallium and bismuth may be frozen in amorphous phases if the substrate temperature is below about 20 K. These data as reproduced in Fig. 24, show that for low substrate temperatures a small stress is developed when the islands join at an average thickness of about 60 Å but no additional stress is produced on further growth. For higher substrate temperatures the usual tensile stress is found. The amorphous Bi films are quite unstable, and with increasing film thickness a spontaneous crystallization often takes place which yields large compressive stresses. These experiments, as well as calculations, convincingly exclude the presumption that the surface temperature of the film is substantiantly higher than the substrate temperature. Because of the present importance of amorphous films, and the general behavior that even alloys seem to grow without intrinsic stress,[106] we report Buckel's result that Sb films condensed on low temperature substrates exhibit rather high tensile stresses. Because the Sb vapor from which the film is built up consists almost completely of Sb_4 molecules, Buckel has reformulated the general hypothesis about amorphous films to read "amorphous phases with a short range order similar to that of a liquid (frozen liquids) grow without internal stress," and interprets the statement on a microscopic void model.

Chaudhari[107] has considered the effect of grain growth on the stresses in films when densification occurs by the elimination of a grain boundary. If the initial grain size is very small a tensile stress is generated and the final grain size is determined by the minimization of the sum of the strain energy and surface energy. When the initial grain size is above this critical

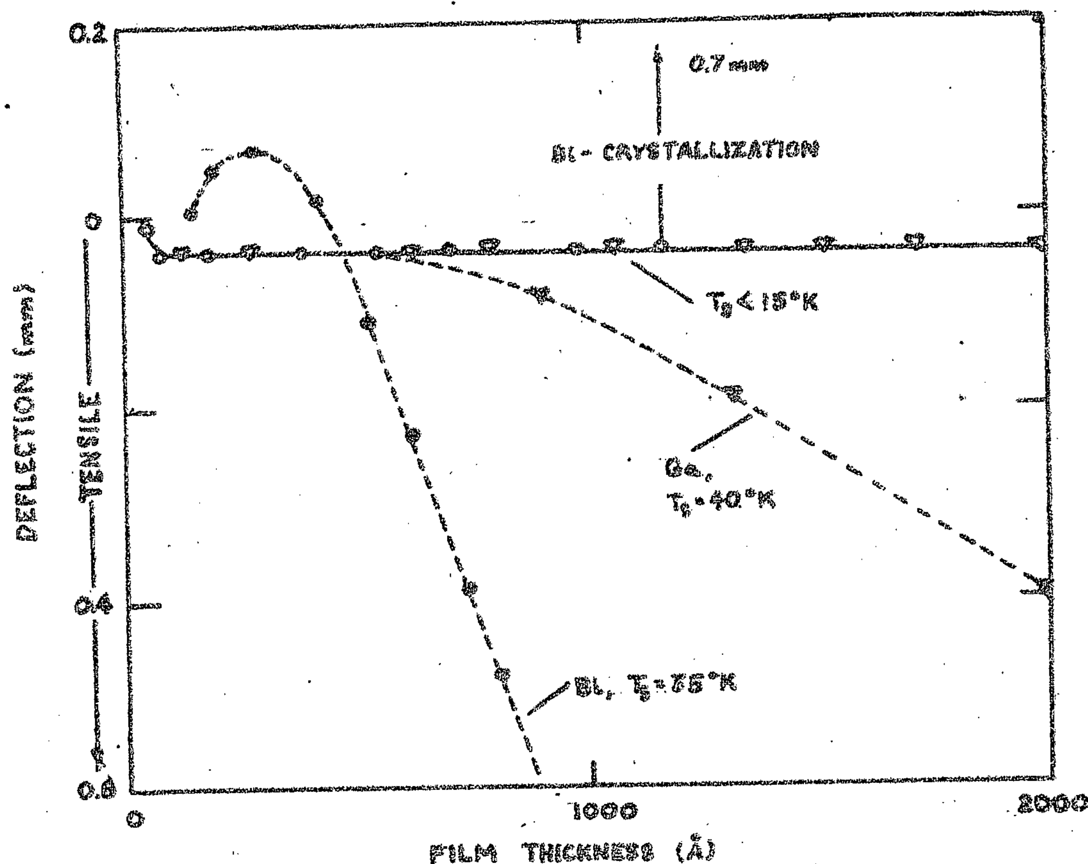

Figure 24. Stresses in low-temperature depositions as measured by Buckel.[8]

size, perhaps 20 Å, no energy minimum is found and grain growth is not restricted. In this model an initial elastic compressive strain aids recrystallization, whereas the experimentally found initial tensile strain is not favorable for grain growth.

Wilcock et al.,[108] have determined the stress in the early growth stage for Ag and A They also consider the stress to arise from the elimination of grain boundaries and suggest only

10% of its boundary need be eliminated to account for the observed stress.

In a series of papers Hoffman[30,32,40] and his coworkers have developed a different concept of a grain boundary model. In this model this strain is generated as the adjacent surfaces of two grains come into contact during growth. The problem may be formulated in terms of a grain boundary potential but this is formally

equivalent to relating the strain energy to the difference between the surface energy of the two crystallites and the energy of the resultant grain boundary. In addition to values of elastic constants and energies this model needs only a value of the final grain size of the film for a quantitative calculation.

The grain boundary potential is demonstrated in Fig. 25. The depth of the potential is given by $2\gamma_{sv}-\gamma_{gb}$ where γ_{sv} is the surface free energy and γ_{gb} the grain boundary energy. As an average grain barely has an energy $\sim \gamma_{sv}/3$, the depth of the potential is $5/3\ \gamma_{sv}$ at the nearest neighbor distance a. An arriving atom may populate any position where the potential is negative if it lies between r and a then the atom relaxes outwards; if it arrives at a position between a and 2a, then a contraction will take place at the boundary. In both cases a strain energy is produced, and the minimum produced between the strain energy and potential energy defines the net strain. As the potential is asymmetric a tension in the film is produced.

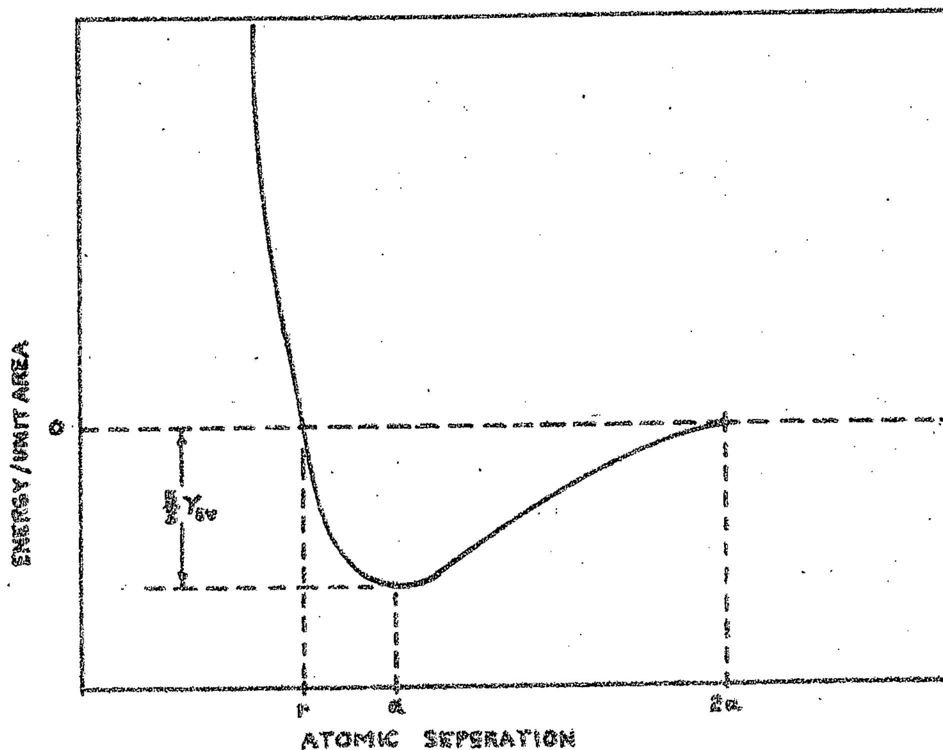

Figure 25. Grain boundary potential. After Doljack, Springer, and Hoffman.

$$\langle\sigma\rangle = \frac{E_f}{1-\nu_f}\frac{\langle\Delta\rangle}{d}$$

where the average displacement $\langle\Delta\rangle$ is obtained by integrating over the range of the potential. Good agreement has been obtained in both the temperature dependence and the magnitude for the case of nickel.[40]

Classification 5, voids and special dislocation arrays, becomes a convenient catch-all. Voids in films have been postulated to explain magnetic anisotropy and low values of density,[109,110] even though the x-ray density is typical of bulk material. With dielectric films evaporated at angles of incidence, voids are popular in order to explain the so-called porousity of the film. Nevertheless, detailed experiments to show the size and shape of such voids have usually failed. The same kind of general remark may be made about dislocations because there is a well-defined stress field around a given dislocation. We may postulate a special dislocation array in order to give rise to any stress distribution that we desire. However, with the exception of the interfacial dislocations mentioned earlier, the dislocation lines found in films by electron diffraction are generally normal to the plane of the film. Thus, generalized statements relative to voids and dislocations, are generally of little use in detailed analysis of the stress problem. Exceptions to this may be found in the case of stacking faults, and other such documented defects in a particular film in question. Abrahams et al.,[111] have proposed an oriented array of inclined dislocations to explain the stress gradient that curls a film upon removal from the substrate. Saito et al.,[112] have postulated a periodic distribution of screw and edge dislocations obliquely piercing the film plus added terms to have a traction-free surface. The maximum stress does not occur at the boundary of the dislocation.

Category 6, contains the expected first-order phase transformation with its attended volume change that must take place after the film is formed for a stress to be generated. Buckel[8] using the Oswald step rule of crystal growth, suggests the film may pass through metastable liquid phase during condensation, and the internal stresses thus arise from a different in density from the liquid itself. Thus, one would expect that a frozen in liquid as the first phase formed exhibits no internal stress, consistent with many results already presented for amorphous metals. As most metals melt with a decreased density, normally a tensile stress will be observed, and this is also experimentally found. Amorphous alloy films also show a very low stress.[106] This model has had some success in predicting the sign of the stress but as yet has not been formulated in a quantitative fashion.

Without specifically stating, our discussion so far has led one to believe that the intrinsic stresses would be isotropic in the plane of the film for randomly oriented polycrystalline samples where the elastic constants are isotropic. The experience with metals has indicated that this is true when the films are deposited at normal incidence. Stress differences of perhaps 20% are found for metals when the evaporated beam is incident at 45° with respect to the substrate normal.[113] These early experiments with magnetic metals were concerned with the anisotropies resulting from the anistropic stress. Smith et al.,[110] suggested that the anisotropy arises during the film growth from a random nucleation in combination with some shadowing effects. This mechanism very likely operates for specimens deposited near grazing incidence but Hoffman and coworkers suggested that anisotropic nucleation and growth would allow the grain boundary mechanism to operate at smaller angles of incidence. Dielectric films have much larger anisotropy effects as we shall see in a following section.

SECTION V SUMMARY OF THE DATA

Introduction

In view of the fact that the importance of the stresses has been known for such a long time, it is surprising that so few papers giving data exist in the literature. Even today the pioneering work of Turner and Truby,[114] Heavens,[115] and Smith, Blackburn, Campbell,[116] Ennos,[42] Carpenter and Campbell,[95] Kinosita *et al.*,[117] and Scheuerman[10] contain perhaps 3/4 of the films studied if we exclude the epitaxial situation. In examining even the recent papers it is still true that improper expressions have been used to relate the stress to the observed parameters, and sufficient information is seldom given to separate the thermal stress from the intrinsic stress. As it is the total stress which affects a given property, this practice may be excused if one is interested in a particular processing treatment, but certainly an understanding of the origin of the intrinsic stresses is not aided by such experiments.

In order to focus our attention let us classify materials as optical films, alkali halides, epitaxial films, and films which perform a passivation, isolation or dielectric function. It will be realized, of course, this is not an all inclusive way of classifying non-metallic films, and furthermore, a number of redundancies will occur when we look at an actual material. The purpose in this classification is to see if there are generalizations we can make within each category which prove useful in trying to interpret the data. Table II contains an updated list following the earlier tabulations of Hoffman,[4] Campbell[7] and Scheuerman.[10] When

only one author made measurements for a particular material, it was simple to quote a value for the stress. Now that several authors have reported for the same material, but often carrying out the deposition at different temperatures or different techniques, there may be considerable disagreement as to the magnitude of the stress and, in some cases, even the sign. Thus, the individual papers must be consulted to see if the conditions of the reader's interest match with those of the literature. We wish to again caution that the intrinsic stress is indeed a structure sensitive property, and seldom is the complete characterization of the film carried out with sufficient detail that such a cause and effect relationship can be found. It is well known that there are significant effects from the ambient atmosphere when a film is taken from vacuum surroundings and that there are longer time effects associated with diffusion of impurities along grain boundaries or through the lattice. Although a few recrystallization studies have been reported, in general stress data is not available for post-deposition treatments.

We have also eliminated consideration in Table II stresses induced in materials as the result of ion implantation as these are not inherently a thin film effect, although measured by the same techniques. There is no question that the incorporation of impurity atoms during sputtering or ion beam deposition can lead to the same kind of behavior, and some of these data are included and will be discussed. We have also eliminated from consideration the growth stresses in what are commonly called "oxide scales on metals". These predominatly thermally-grown oxides, a subfield in themselves, have been reviewed in considerable detail by Stringer.[82] Likewise we have excluded anodic oxides.

After this rather lengthy introduction we turn now to the data for optical films. A general review of optical films by Ritter[103] will appear soon and laser window coatings have been reviewed by Young.[104] The average stress is generally displayed as a function of thickness, in some cases the force per unit width or its derivative is plotted. The average stress usually increases rapidly, reaching a maximum value at a thickness of a few hundred anstroms, and then becomes a slowly decreasing function of the thickness as indicated in Fig. 26 for several materials. For films deposited in a liquid-nitrogen trapped diffusion pump system at pressures of about 10^{-4} Pascal, Ennos[42] finds a significant increase in tensile stress with a time constant of about 100 seconds after the deposition is stopped. This transient very likely results from thermal relaxation of the substrate although the author experimentally found no initial transient. Significant transients are also found when the film is exposed to air over a period of perhaps 30 minutes.

TABLE II

Index to Stress Literature

Film	Substrate	Reference
AgCl	Glass	114
AgF	Glass	114
AgI	Glass	114
AlPh*	Glass	116
AlF_3	Glass	114
Al_2O_3	Al	159
	Si	54, 163, 164
	Silica	10
B_2O_3	Glass	116
BaF_2	Glass	114
BaO	Glass	116
C	Glass	131
CaF_2	Glass	114, 116
	Mica	115
	Silica	42
CdS	Glass	116
CdTe	Mica	165
	Silica	10, 42
CeF_3	Glass	116
	Silica	42
Ce_2O_3	Glass	114
	Silica	42
Chiolite	Glass	114
	Silica	42
Cryolite	Glass	114, 115, 132
	Silica	42
CuI	Glass	114, 157
Fe_3Si	Fe	162
Ge	Silica	10, 42
	Glass	56
	Mica	166
KBr	Glass	95

*Ph = phthalocyanine

TABLE II (con't)

Film	Substrate	Reference
KCl	Glass	95
KF	Glass	95
KI	Glass	95
LiF	Carbon on glass	134
	Cellulose	135
	Glass	95, 114, 116, 131, 132, 134
	Mica	115
MgF_2	Glass	114, 116, 132, 136, 143
	Mica	115, 117, 137
	Silica	42, 151
MgO	Silica	10
MgPh*	Glass	116
MoO_3	Glass	114
NaBr	Glass	95
NaCl	Glass	95
NaF	Glass	95, 132
$PbCl_2$	Glass	114, 116
	Silica	42
PbF_2	Glass	116
PbTe	Glass	138
	Mica	138
RbI	Glass	95
Sb_2O_3	Glass	114
Sb_2S_3	Glass	114
Si	Sapphire	59, 78, 123, 124
	Quartz	71
	Si	59
	Spinel	33, 77
Si_3N_4	Si	48, 128, 129, 158
SiO	Glass	116, 122, 134, 139, 140, 141, 142, 144, 145
	Nickel	146
	Silica	10, 42
	Al	161
Glass	W	133

*Ph - phthalocyanine

TABLE II (con't)

Film	Substrate	Reference
SiO_2 (CVD)	Si	67, 148, 160
SiO_2 (Sputtered)	Si	55, 67, 148, 149, 164
SiO_2 (Reactive Evap)	Si	153
	Silica	10, 152
SiO_2 (Thermal Decomposition)	Si	149
	Ge	149
SiO_2 (Thermal Oxide)	Si	10, 51, 52, 53, 54, 67, 127, 148, 149
SiO_xN_y	Glass	153
	Si	130, 158
SnO_2	Glass	114
$SrSo_4$	Glass	114
TaO_x	Ta	154
Ta_2O_5	Ta	155, 156
	Glass	156
Te	Silica	10
TiO_2	Glass	153
TlCe	Silica	42
TlI	Silica	42
ThF_4	Silica	10, 42, 152
($ThOF_2$)	Silica	147
ThO_2	Silica	10
ZnS	Glass	114, 116
	Mica	115, 117
	Silica	10, 42, 147, 152
ZrO_2	Silica	10

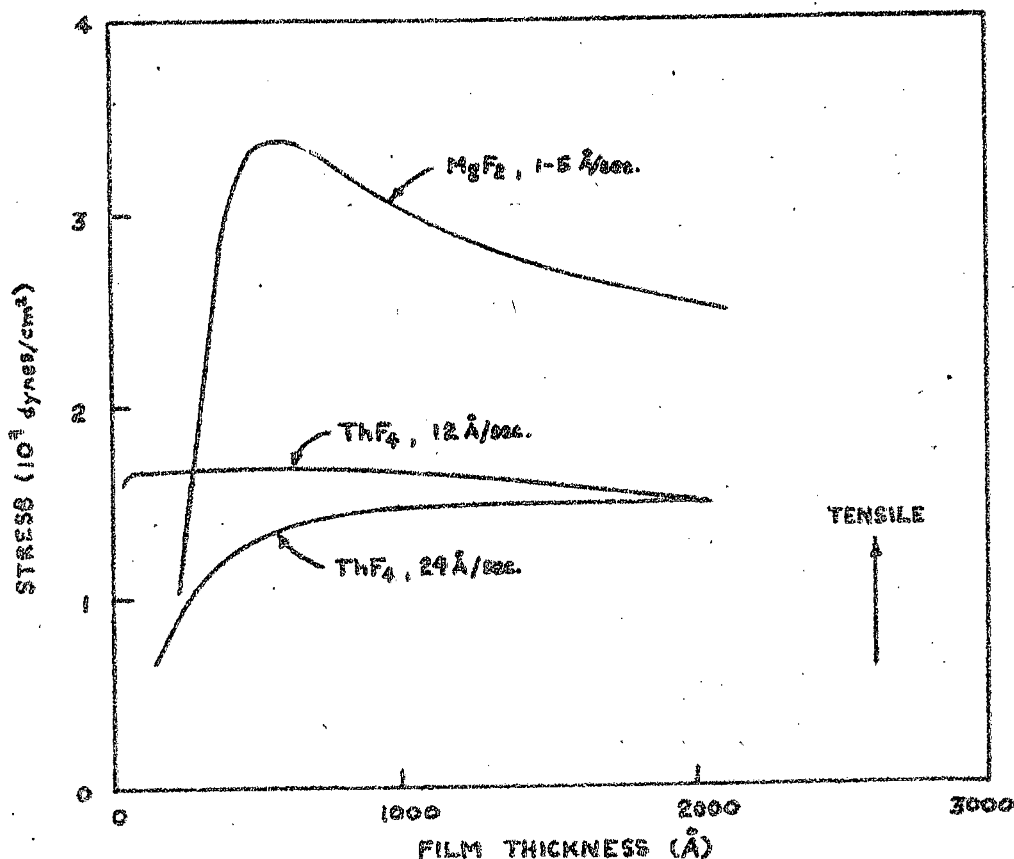

Figure 26. Representative data for the stress in optical films. From Ennos.[42]

Of the common optical materials only ZnS is deposited under compression, although Kinosita et al.,[117] indicate that a tensile stress may be found for low deposition rates. Fig. 27 summarizes some of these results for ZnS and it is interesting to point out that for the same deposition rate, data from different laboratories can be obtained which are most a negative of each other. Blackburn and Campbell[46] have found a linear increase in the compressive stress in ZnS films with the increasing rate of deposition in the range of 5 to 30 A/sec. The intrinsic stress in ZnS is also a rapidly decreasing function as a substrate temperature is raised from 80 to 150° C.

These differences point out the subtleties in the dependence of the stress on the deposition conditions. It is known[118] that the evaporation geometry, especially as related to the self-gettering is important for determining the morphology. ED, SIMS, index of

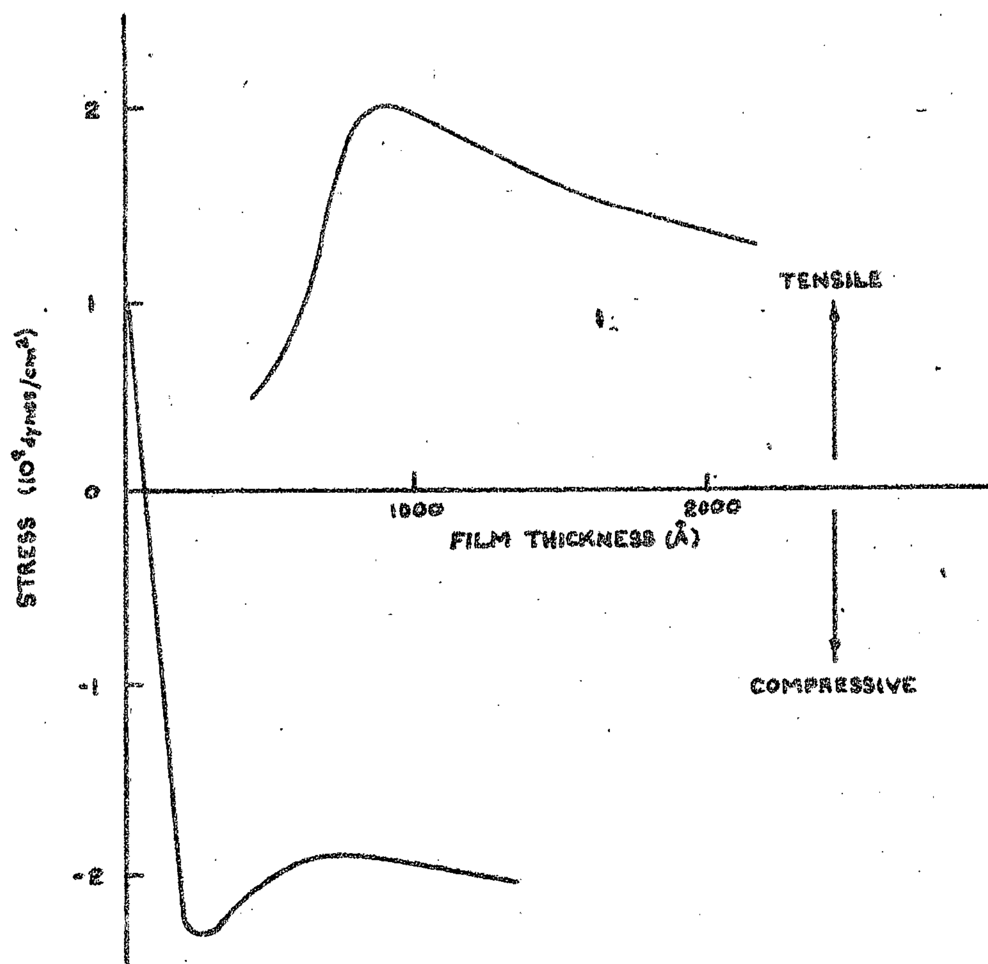

Figure 27. Stress in ZnS films. Tensile data from Kinosita et al.[117] Compression from Ennos.[42]

refraction, and density measurements have recently been made for ZnS by Preisinger and Pulker.[119] The columnar crystallites have a diameter which slowly increases with thickness above 500 A. The non-stoichiometric excess of S was found to be due to S_2^- bound to the surfaces of the crystallite columns.

Pulker and Jung[120] have suggested a cylindrical column model for the structure of ZnS and other optical films based on electron microscopy and water vapor absorption data. The observations suggest that an explanation for the stress might be sought in the impurity-grain boundary model.

Hill and G. R. Hoffman[122] have made an extensive evaluation of silicon monoxide. In the first place, they find a linear force-thickness curve for constant evaporation conditions, suggesting that some of the behavior for thin films less than 1000Å thick may result in the difficulty in establishing steady-state conditions. Furthermore, they establish that the stress is a sensitive function of the residual gasses when the arriving silicon monoxide flux is comparable in magnitude. That the stress was indeed a function of the atmosphere during deposition, was strikingly demonstrated by changing the atmosphere during deposition with the resultant change in the sign of the stress in the material being deposited. Their data is summarized in Fig. 28 where the stress is plotted against the logarithm of the ratio, N, of the arrival rate of silicon monoxide to residual gas molecules at the substrate. Dielectric constant measurements suggest that the tensile stress occurring when the ratio N > 1 may be thought of as the intrinsic stress of silicon monoxide, whereas increasing the pressure of oxygen results in a silicon dioxide deposit. The earlier source tempera-

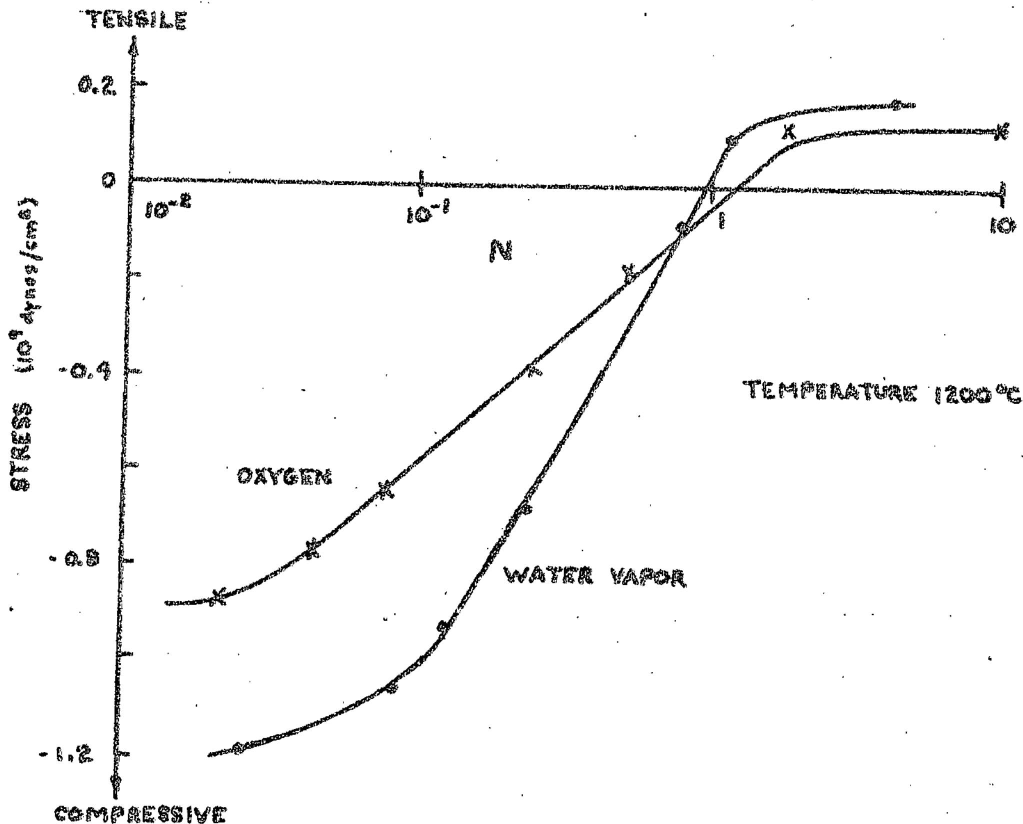

Figure 28. Stress in SiO films as a function of SiO to O arrival rate. After Hill and Hoffman.[122]

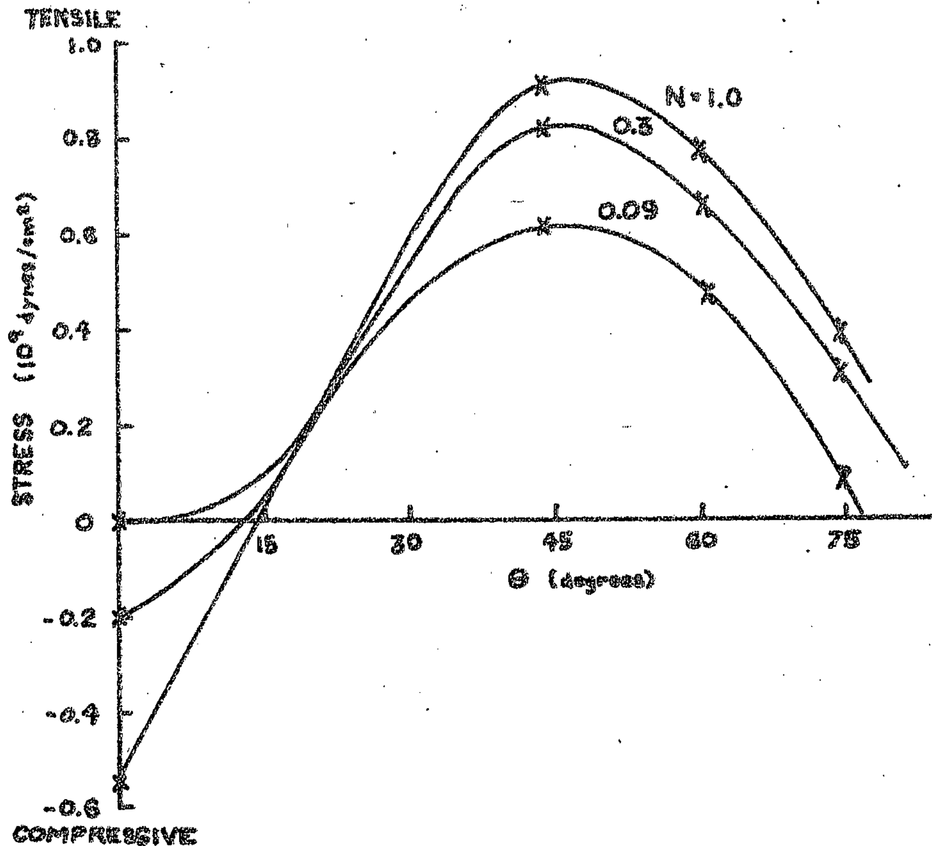

Figure 29. Angle of incidence effects in SiO. After Hill and Hoffman.[122]

ture dependence found by Novice and Priest and his co-workers may now be understood in terms of the ratio N. Furthermore, these results confirm the earlier rate and residual gas pressure measurements of Blackburn and Campbell.[116]

Hill and Hoffman also report that the film stress remains stable as long as the specimen is under vacuum, but on the readmission of atmosphere the stress becomes more compressive, independent of its initial value. The increase in compression upon exposure to ambient may be several times the initial compressive stress, and to explain this fact they suggest that such films have a low density which makes them more susceptible to oxidation.

Hill and Hoffman have investigated angle of incidence effects where there is a dramatic increase in the tendency to form films in tension near 45° incidence even under oxidizing conditions (Fig. 29). At the same time an enhanced compressive change results upon exposure to the atmosphere. These results are in

general agreement with the earlier ones of Priest *et al.*,[181] in which the stress anisotropy was measured using two orthogonal substrates, and again emphasize the sizeable morphological changes at modest angles of incidence.

Hodgkinson and Walker[210] have irradiated SiO films with ultraviolet and found that prolonged irradiation in vacuum will change the initial compression to tension, but the stress reverts back to compression when air is admitted. Films irradiated in air also had a substantial reduction in the compressive stress, and related changes in refractive index and UV optical absorption. The stress changes under irradiation are associated with the rearrangement of oxygen already gettered during the deposition with a resultant tensile contribution which partly counteracts the existing compression.

Although the data for other optical films is less complete, we suggest that the purer the film the greater the tendency for tension, and oxygen or other impurities tend to give compressive contributions.

The intrinsic stress in alkali halide films has been investigated by Carpenter and Campbell.[95] Data in the form of force and average stress as a function of thickness are presented for many of the alkali halides. Lithium salts show tension and potassium salts compression throughout the thickness range covered. Sodium salts have a large compression below a thickness of 1000 Å and a tension above. The common features exhibited by all the curves are a stress maximum which is usually compressive and occurs at a thickness of about 250 Å and a constant stress region for thicknesses greater than about 1000 Å, with a relative insensitivity to deposition rate. LiF has been studied by a number of investigators as summarized in Table II. Carpenter and Campbell point out that there appear to be two different stress producing mechanisms and suggest a misfit model for the first stage, even though the substrates were soda-lime glass. The average stress as a function of lattice constant as plotted in Fig. 30 goes through zero at the oxygen nearest-neighbor distance in the glass. Although surface tension contributions may contribute to the stress in this isolated island stage of growth it is not possible to explain the systematic behavior shown in the figure on this basis. No satisfactory explanation has been made for the intrinsic stress in thicker films.

Rather than to try to review the entire literature relative to epitaxial films, we consider a few illustrative examples. When the film is very thin or consists of small nuclei, a uniform elastic strain is predicted and has been observed for metals. The introduction of misfit dislocations to reduce the total energy localizes the strain at the interface. This problem has been treated in various formulations by Van der Merwe and his colleagues and discussed earlier. However, the fact that many epitaxial films are deposited at high temperatures and then observed at room temperature means that the thermal stresses are also often very large even though care is usually taken to minimize the stress gradient near the interface may be especially important in determining properties which are sensitive to that region it is often not the major contribution to the total stress in a thicker film. One should really ask the question, "are there any data for the

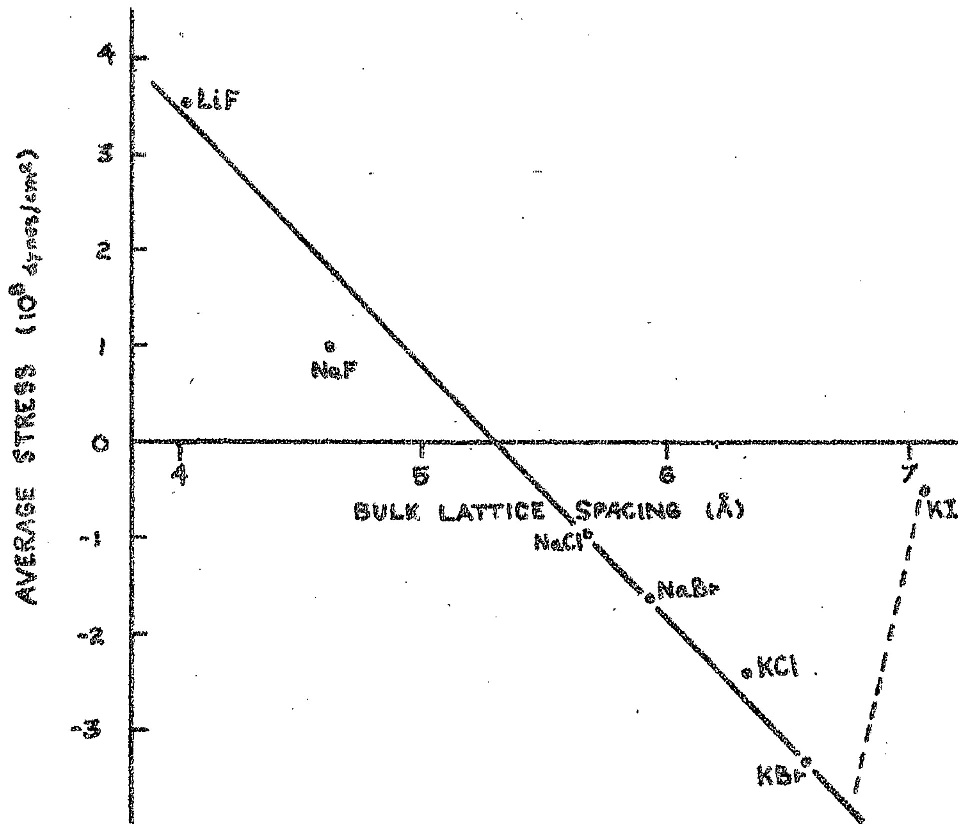

Figure 30. Average stress in very thin alkali halide films correlates with epitaxial effect on glass substrates. After Carpenter and Campbell.[95]

stress in epitaxially grown films that require the presence of a volume intrinsic stress". This is a difficult experimental question to answer. First of all, the intrinsic stress is generally a decreasing function of the substrate temperature and is likely to be very small at elevated temperatures. And, secondly, relaxation processes undoubtedly operate which may prevent an intrinsic stress, if generated, from being observed. Dumin,[123] in the case of silicon on sapphire, was not able to obtain the necessary precision. Other workers,[124,59,78] have also found large compressive stresses ($\sim 10^{10}$ dynes/cm^2) for the Si/Al_2O_3 system. Kamins and Meieran find if the epitaxial films are electrolytically stripped from the substrates the constraint is lifted and the strain is reduced to a level equal to the resolution limit of the diffractometer technique. In every case, thermal

expansion is sufficient to account for the compression. Dumin does not mention any stress anisotropy, Kamins and Meieran, using a diffractometer technique, mention but cannot measure an anisotropy, and Hughes and Thorsen calculate the stress anisotropy resulting from the anisotropic thermal expansion and confirm it by mobility measurements.

In the case of silicon on spinel, larger compressive stresses were observed. Schlötterer[77] found isotropic stresses while Robinson and Dumin[33] notice anisotropic deformations, again with the magnitude close to that expected from a thermal origin. The recent stress birefringence measurements of Rinehart and Logan[73] on $Al_x Ga_{(1-x)}$/GaAs structures also indicate that the thermal expansion stress dominates the room temperature stress situation.

The epitaxial garnet films also represent a well-studied system because of their use in bubble devices. Zeyfang,[125] using a double crystal diffractometer concluded the thermal stress operated in YIG on YAG.
Many examples are presented by Besser et al.,[96] clearing up previous inconsistencies in understanding the crazing associated with these films. Broginski et al.,[98] conclude the mismatch stresses are of prime importance for YIG films on $Gd_{3-x} Dy_x Ga_5O_{12}$ substrates as a result of magnetic anisotropy field measurements. They propose a balance between the thermal expansion stresses and the misfit dislocations to explain the almost zero stress at large values of x. As described earlier Carruthers[97] has extended these concepts to a partial relaxation.

In summary, thermal and misfit contributions seem sufficient to explain epitaxial stresses for the cases in the present literature.

In order to account for the bending that deposited epitaxial films undergo after separation from the substrate, Abrahams et al.,[111] had suggested an oriented array of inclined dislocations. For films for $GaAs_{1-x}$ on GaAs, they found a correlation between the number of inclined dislocations, the lattice mismatch, and the amount of bending. An alternative explanation of this well-known bending phenomenon was attributed to the misfit dislocations near the interface. As a stress gradient through the thickness of the film is needed to account for the curling, the criticism of Abrahams et al., that misfit dislocations should apply only to 100 Å layers is not valid.

We consider now the last category, namely, films used for insulating, passavating, or isolation purposes. This area is, of course, of extreme importance to the technology of thin films. We regard the electrical effects of such films beyond the scope of this article and content ourselves with some general considera-

tions concerning the mechanical properties. There is a review by Pliskin et al.,[126] on thin glass films and Dell'oca et al.,[84] consider anodic layers. As the glass films are generally applied on heated substrates, and glass as a material is stronger under compression, one desires the total stress in the film to be compressive at the operating temperature. Thermally grown SiO_2 has perhaps received the most attention. But here the substrate is at high temperatures during the formation of the film and there is only modest control over the resultant compressive stress

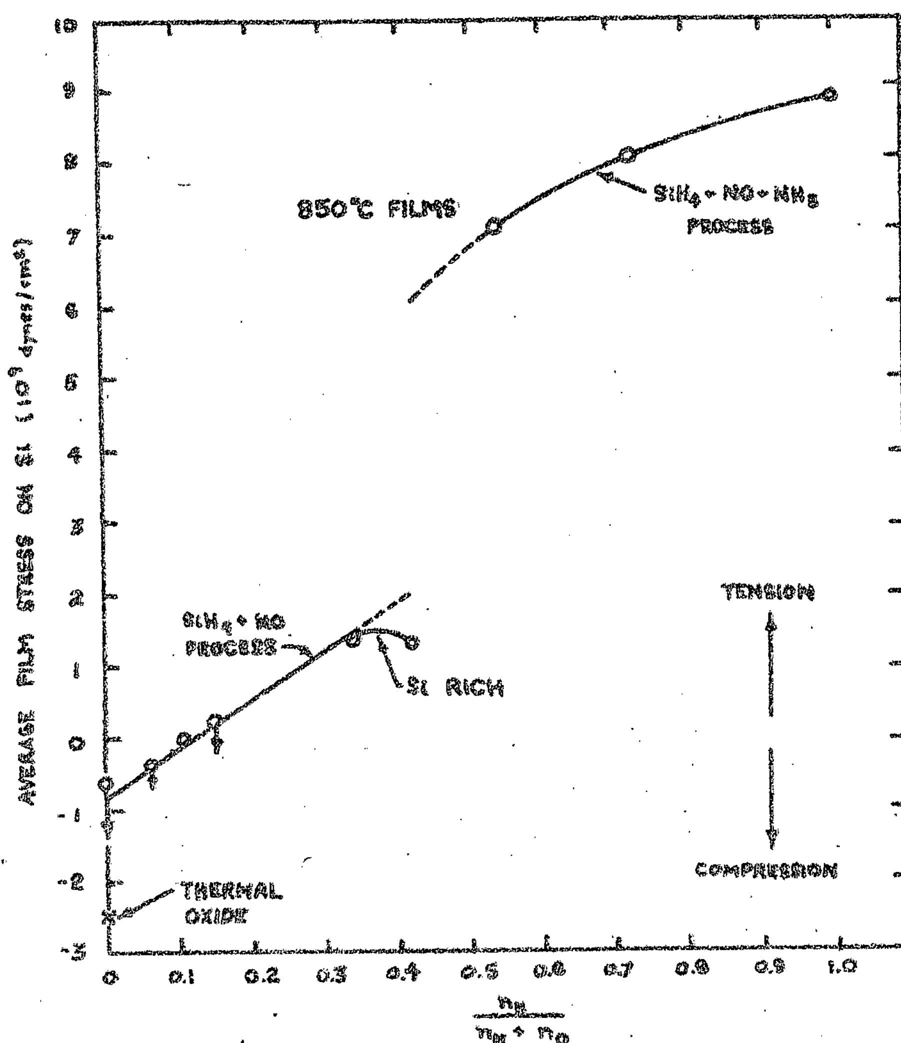

Figure 31. Average stress in silicon oxynitride films as a function of nitride composition. From Rand and Roberts.[130]

($\sim 3 \times 10^9$ dyne/cm^2) as the temperature range to form the oxide is limited, and wet or dry oxidation makes only a small difference.[51,127] Most authors report no thickness dependence in the range of 0.5 - 2 μm. However, a rapidly increasing compression at small thicknesses is found by Lin and Pugacz-Moraszkiewiez[53] in the range 0.1 - 0.3 μm. Thermal mismatch is recognized as the origin for thermally grown oxides, but intrinsic mechanisms are reported for CVD SiO_2 films deposited at somewhat lower temperatures[148] when the total stress is about 2×10^9 dyne/cm^2 tension. Post deposition heat treatments change the stress back to compression. A tensile intrinsic stress is also found in the case of thermal decomposition of tetraethylorothosilicates.[149]

More recently Si_3N_4[128,129] has been used as a passavation layer for Si. In this case an extremely large intrinsic stress of $> 1 \times 10^{10}$ dyne/cm tension is found coupled with thermal stresses of perhaps 10% of the total. The stress does not change with time. Rand and Roberts[130] report amorphous silicon oxynitride films that range in value from almost that of the thermal oxide compression to the large tension of Si_3N_4 as the nitride concentration increases as shown in Fig. 31. These large stresses in both SiO_2 and Si_3N_4 can damage the substrate as we shall see in the next sections.

Although the intrinsic stress rapidly decreases with increasing substrate temperature in metals, we see that substantial intrinsic stresses are present for CVD insulation films.

We try to summarize the literature for non-metallic films as follows:

1. Although thermal contributions may be large, intrinsic stresses are well documented in both polycrystalline and epitaxial films.

2. Real stress contributions have been seen during the isolated island stage of growth, but these contributions should no longer dominate at average film thicknesses of perhaps two hundred angstroms and are often masked by poor thermal control in the experiment.

3. There is a tendency for stress values to be tensile in polycrystalline films independent of thickness when the deposition parameters are well defined. This suggests that the major contribution to the intrinsic stress in thick films is a volume effect and not an interfacial one. Further, for pure films the stress should be capable of an explanation by similar models as those developed for metals.

4. Compressional contributions are associated with impurities, often oxygen, incorporated in the structure by design or default. These may take place during deposition, or afterward by diffusion. Non-stiochiometric films may also show compression.

5. The decrease in the average stress as the thickness increases may result from a relief process or a change in the intrinsic stress mechanism. The present measurements are not sufficiently complete to generalize, but on energetic grounds a relief mechanism must ultimately operate. Cracking in film or damage to the substrate may result.

6. Both thermal and misfit contributions operate in epitaxial films. The intrinsic contributions are amenable to calculation, and may be either a uniform elastic strain or localized at the substrate interface.

SECTION VI. CONTROL OF STRESSES, INCLUDING RELAXATION EFFECTS

One of the objectives of understanding the intrinsic stresses in films is to be able to control the stresses and hence the properties for a given application. As we have seen, considerable progress has been made in the case of epitaxial systems. Recently for the case of metals stress control has come about by the use of bias sputtering. Blachman,[150,151] in the case of molybdenum and aluminum, has found a correlation between the stress resistivity and trapped argon content. With increasing negative bias substantial amounts of gas are entrapped which reduce the tension in the film or may even change it to compression. On the other hand, Sun et al.,[167] for the case of sputtered tungsten, find a sizeable compression which is not correlated with the argon concentration. In a following paper[209] they find a strong correlation with final grain size in the W films. The structure and stress modifications by ion bomardment during deposition have been studied by Maddox and his co-workers.[168,169,170] Stuart[154] has used the cantilever method to measure the stress in a number of metals deposited by low pressure triode sputtering. Data for the non-metals is not so common, but it appears that one can change the bias to substantially modify the stress even in these systems. We also call attention to the UV irradiation effects mentioned earlier.[210]

The use of elevated substrate temperatures to reduce the intrinsic stress among other things, has been done for a long time. In addition it is sometimes possible to provide a thermal contribution which gives cancellation with intrinsic stress mechanisms by the proper choice of substrate.

Post-deposition treatments may reduce the stress, as it has been known for a some in films of metals deposited at lower substrate temperatures that stress relief mechanisms operate upon heating the substrate to elevated temperatures.[171] Resistivity and stress changes have been correlated and activation energy measurements made[172] which indicate that very likely a simple defect motion at lower temperatures is followed by recrystallization Such irreversible changes upon initial heating are usually followed by reversible behavior upon temperatures cycling at lower temperatures. Chaudhari[21] has considered the mechanisms of stress relief in polycrystalline films. Dislocation sources within a grain at a grain boundary or at surfaces are not likely mechanisms because the stress required to operate such dislocation sources is larger than the usual intrinsic stresses within a film. To a first approximation the stress necessary to operate sources varies inversely with the diameter of the grain as shown in Fig. 32. A similar result is observed

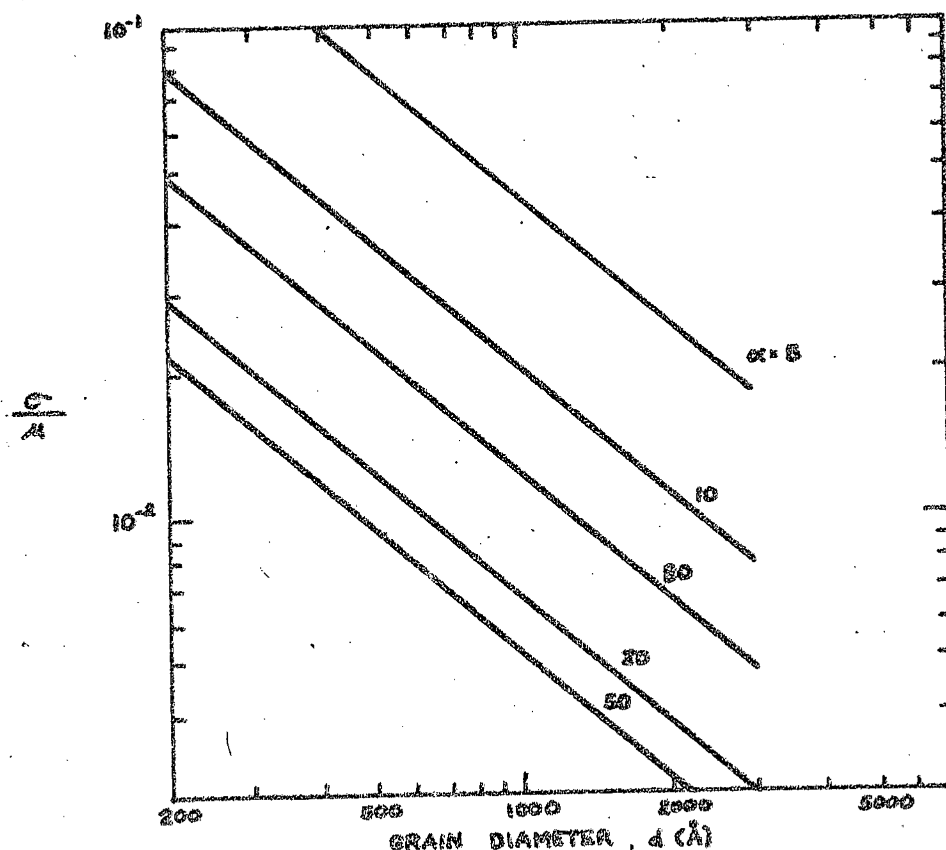

Figure 32. Critical stress to operate a dislocation source as a function of grain diameter for several inclinations. After Chaudhari.[21]

for sources at a grain boundary ledge, but since the intrinsic stresses are the order of 10^{-2} of the shear modulus, these processes are not normally favored. Kinetic equations for the exponential relaxation of the stress on a grain boundary sliding model were also derived by Chaudhari. As most grain boundaries in a film are perpendicular to a free surface under a planar biaxial stress the shear stress acting on the boundary is small and hence the plastic strain contribution from grain boundaries sliding is expected to be small. The annealing kinetics have been derived for diffusional creep for the cases of volume difusion and grain boundary diffusion predominating. In this case the thickness of the film matters and of course the activation energies for the two hypotheses are different. Although these equations were derived for the case of a uniform stress, it is pointed out that stress gradients also provide an additional driving force. If a stressed film is covered by a diffusion barrier containing a hole, the film relieves its elastic strains by a flow of matter between the surface and interior of the film. Mass flows out of the film under a compressive stress and into a film under tensile stress, leaving a hillock or depression. Pennabacker[173] has also considered that compressive stresses lead to hillock growth. Chaudhari[174] has recently calculated the hillock density and growth kinetics on the basis of a local relaxation of a compressive stress.

For the case of growing oxide films, Stringer[82] has considered additional mechanisms for plastic flow. The effect of stoichiometry on the oxide plasticity and the reasons for suggesting plastic flow takes place during oxidation are discussed. In addition, vacancy injection and dislocation generation at the metal substrate are examined. A more direct measurement of stress enhanced diffusion in thin films was given by Gangulee[175] in which Be atoms diffuse along grain boundaries of Al films and along the interface between the film and oxidized silicon substrate at a considerably enhanced rate when a tensile stress is applied to the plane of the film.

Diffusion may also be a source of strain. Takai and Francombe[176] have measured a cantilevered deflection during the interdiffusion of gold and aluminum both an increase in stress corresponding to the growth of intermetallic compound faces and stress relief were noted. Tu et al.,[137] have studied the Ni-Si system and Lau and Sun[177] the interdiffusion of Ti-Pd-Au films.

Similar cases of enhanced migration are commonly found in the recrystallization of amorphous layers of silicon which are produced by ion bombardment of an aluminum coated silicon substrate. Silicon is transported to the surface of the thin aluminum surface according to Hart, et al.[178,179] Additional low

temperature rapid migrations have also been found, and this subject has been treated in a recent conference,[180] in which both review papers and research reports will be found.

Helium implanted erbium films examined by Blewer and Maurin[181] have shown dimensional expansion at the surface and microscopic bubbles formed at the surface by the release of helium by the films. Additional dilation data is found in the semiconductor literature.

Stress annealing data for non-metallic films is not common. In the case of silicon monoxide Priest and Caswell[146] showed that no stress change took place with a low temperature anneal in vacuum. But as soon as the pressures of oxygen or water vapor exceeded about 10^{-3} Pascal, rapid compressive changes took place. This is, of course, related to the degree of oxidation as was discussed earlier and we would anticipate that the changes often found when optical films are exposed to the atmosphere, have a related origin. Mattox and Kominiak[168] annealed bias sputtered Corning 1720 glass films at low temperatures. The initial compressive stress became larger, and at temperatures above about 350° the films showed a total tension. This irreversible behavior was again traced to an oxygen deficiency.

At the present time, it is well documented that grain boundary diffusion plays an almost dominant role in small-grained films, even though both lattice and diffusion down dislocation pipes may take place in special circumstances of large grain size, or extreme dislocation concentrations. Nevertheless, the detailed kinetics, especially in the case of impurity diffusion, are the subject of present investigations. The resultant stress relaxations are less well understood, and even the detailed mechanisms are still in doubt for metals,[3] and almost unknown for non-metals.

VII. MODULI, FAILURE MODES AND ADHESION

We should comment on the values of elastic modulii for deposited films. Although occasionally low values are found, as reviewed by Hoffman,[4] most films when carefully measured show the expected values of the modulii. In addition to direct deflection measurement, resonance techniques[108,182,183] have been used. Spinner[184,185] used a dynamic technique to measure the moduli of many glasses as a function of temperature. Uozumi et al.,[186] have used the pulse-echo technique and sound velocity to determine the modulii. In view of the present interest in amorphous solids we call attention to the work by Chen and Wang, and emphasized by Berry and Pritchet[182] there is a growing body of evidence that Young's modulus for materials in the amorphous state may be characteristically 20 - 40% below the value in the crystalline state. Merz et al.[211] found a 45% decrease in the shear constant of $Sm_2 Co_{17}$ sputtered alloy, but only a 7% decrease in the bulk modulus compared to the crystalline phase. These measurements support the ideas of Weaire et al.[212] that microscopic internal movements take place in amorphous materials under shear.

We would expect similar changes in the amorphous layer induced in silicon by ion implantation.[188] Internal friction measurements have given information as to loss mechanisms and thermal constants[182,186].

Bunshah,[189] has reviewed the properties of evaporated thick films and correlated the mechanical properties of thick, primarily metallic, films were reported in the Conferences on Structure/ Property relationships in Thick Films and Bulk Coatings.[190]

Kinosita[9] has reported unexpected microhardness measurements for LiF thin films with a Vicker-type indenter, and Winter[191] has developed apparatus for similar measurements using both an indenter and impact from spherical projectiles.

We consider now an outline of the failure modes, which may range from a mechanical distortion of an optical surface,[152] through drastically changed properties, especially near the interface as indicated in several examples. We concentrate here on the obvious mechanical failures of cracking in the film or substrate and buckling if the film has a large compressive stress.

The importance of the adhesion in preventing failure is well known, although quantitative treatments are difficult to find. Hunt and Gale[192] suggested a model of the adherence to stresses in plastic film, in which the lift-off stress normal to the plane of the film is proportional to the gradient of the tension in the film substrate interface. The importance of the edges of the film, or other defects which may be present, is well known and can be explained by the non-uniform stresses near the edges of the film as we mentioned earlier. Plassa,[166] has also studied the elastic instability of germanium films as they buckle from a mica substrate. Random wrinkles are found with an isotropic intrinsic stress although oriented wrinkles were found earlier by Yelon and Voegeli[194] in the case of epitaxial films and a suggestion for the sinusoidal wrinkle pattern in terms of a column instability has been made by Plassa and Chopra[11]. As the stress is generally a volume effect, the total force that must be supported across the interface increases as the film becomes thicker. This leads to a critical failure thickness which is a function of the stress in the film and the adhesion to the substrate. The buckling, of course, results from a film under high compression whereas a cracking will be found for films under sufficiently high tension that the fracture stress is exceeded.

Angle of incidence effects may also produce oriented buckled patterns observed in ZnS by Behrndt[195] which were eliminated by rotating substrates, and we discussed earlier the extreme dependence in the SiO system. Recent emphasis on deposition techniques other than evaporation have eliminated many of these problems.

Dislocation generation and even cracking as a result of the residual elastic strains in epitaxial films is well documented. In the galium arsenide photodiode heteroepitaxy the lattice parameter mismatch had to be graded at a slow rate to avoid excessive dislocation generation. We referred earlier to the stress by refringence and cracking in the magnetic bubble materials. Carruthers[97] has treated the deformation and creep as well as estimating the property changes. It was known that thin dielectric films of the order of 1 μm may accommodate the high stresses normally found, but thicker films are found to crack. Matthews and Klokholm[196] have considered the fracture of these brittle films under the influence of the misfit stress. The cracks that form in the garnet films are perpendicular to the film plane. If such cracks are to propagate through the film, which is rigidly bonded to its substrate and strained in tension, then the film thickness must exceed the Griffith crack length. If the stress exceeds the fracture strength of the crystal then

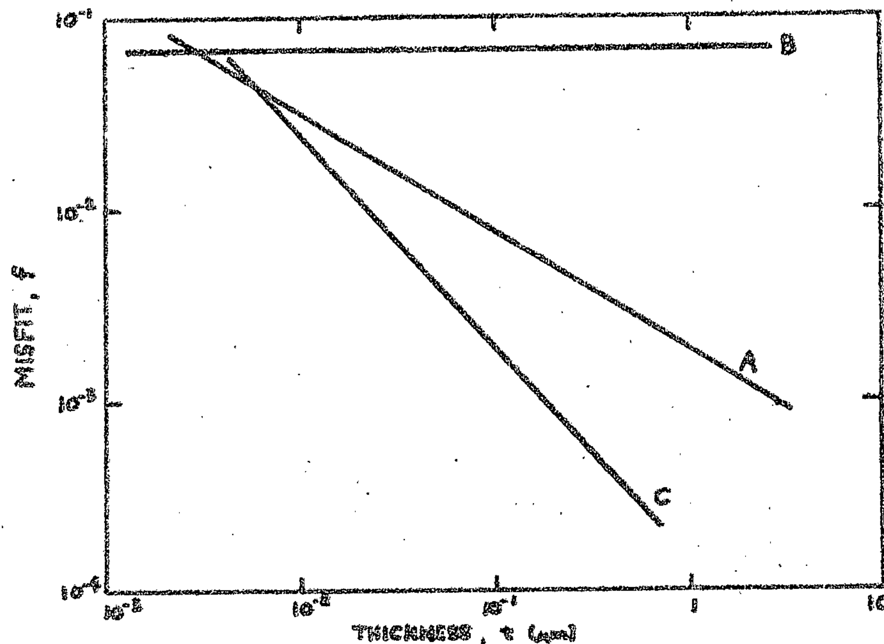

Figure 33. Crack generation in brittle films as a function of misfit and thickness. Above B film spontaneously cracks, below C it is elastically strained and above A cracks will propagate. After Matthews and Klokholm.[196]

a spontaneous fracture will take place, whereas, for a low stress the film may strain elastically and be stable. These results are summarized in Fig. 33 as a function of the misfit. Indeed, the presence of cracks in a film indicates that the density of misfit dislocations lies below the optimum value and indicates there are difficulties associated with the generation of these dislocations.

SiO_2 or Si_3N_4 films are known to develop dislocations or cracks in the underlying silicon substrates. Kato et al., Westdorp and Schwuttke,[128] and Tamura and Sunami[129] have considered this problem in detail. The internal stresses were measured, isothermal annealing treatments were carried out, and the density of dislocations introduced during the high temperature anneal were measured. Dislocations in the garent system have been studied in a series of papers by Matthews and Klokholm.[197]

We finally consider adhesion. Much has been said about adhesion in a qualitative way, but to date, the field still suffers from good measurement techniques. Campbell[7] has reviewed this area well and annual conferences of the subject have been published[198] in Aspects of Adhesion. Techniques in cleaning, depositing thin reactive metal layers to aid bonding to glass, interdiffusion, and grading the composition all have been used to enhance the adhesion. Nevertheless, a detailed understanding of even the origin of the forces is obscure, although Van de Vaals coupling is suggested as the most important contributor with band structure effects being important in clean metal surfaces.[199,200]

The stress distributions in an adhesive layer have been calculated by Harrison and Harrison.[201]

We leave the discussion of the most recent measurement techniques to the recent reviews by Chapman[202] and Kendall[203] and the forthcoming review by Weaver[204] and mention here only deposition techniques which should prove useful as well as a brief report of the surface analysis techniques that may provide some of the quantitative information needed for an understanding.

It has long been known that sputtered films generally have better aherence to a substrate than to evaporated ones. The higher energy of the arriving atoms allows a small penetration and/or a cleaning of the surface. The ion plating technique as pioneered by Mattox carries this process even further by subjecting the substrate to a flux of high energy ion before and during the film deposition. From the point of view of adhesion, several benefits may be obtained. The surface will be sputter cleaned and maintain clean until the film begins to form. The high energy flux to the substrate surface provides a high effec-

tive surface temperature, enhancing diffusion and chemical reaction. The high defect concentration also provides a physical admixing of the film and substrate material. According to Mattox[205] this process gives rise to sizeable gas incorporation. As the negative bias is increased, the gas entrapment decreases again at biases above a few 100 volts, presumably because the high temperature of the deposit allows the gas to diffuse away. Densities of as much as a factor of 2 lower than bulk densities are observed, and the growth morthology is decidedly influenced. As far as the stress is concerned an increase in intrinsic compressive film stress is generally found with increasing negative bias, for metal films.

More recently experimental techniques of AES have been applied to the adhesion question. Stoddart et al.,[206] have studied the effect of the glow discharge on adhesion. Although no surface electrical or topographical effects were seen, gross contamination as well as gas sorption were felt to be important. Houston and Bland[207] found that the discharge current could act as process control variable to indicate a clean cathode surface, if proper care was taken. Westwood and Bennewitz[208] in reactively sputtered PTO films noted that the presence of oxygen was necessary for good adhesion.

It is premature to generalize from the results but it appears as though certain impurities in small concentrations at the interface are beneficial and, in fact, even needed for good adhesion. Sundahl[193] found the presence of Cu and Si on the surface of high purity Al_2O_3 as well as a small grain size in the substrate were important factors. With the increased availability of surface analysis techniques we expect significant progress in understanding adhesion.

ACKNOWLEDGEMENTS

I would like to dedicate this paper to my students, both past and present, who have taught me so much about the mechanical properties. I also wish to thank P. Chaudhari, D. M. Hoffman, A. Kinbara, K. Kinosita, E. Klokholm, S. Mader, E. Ritter, and W. D. Westwood for their helpful discussions and information. Mrs. M. Young and R. Wenz have my gratitude for their faithful efforts in production of the manuscript. The research at Case Western Reserve University was supported by the U. S. Atomic Energy Commission.

REFERENCES

1. See, for example: E. Klokholm, J. Vac. Sci. Tech. 8, 148 (1971).

2. M. H. Francombe, A. J. Noreika, W. J. Takei, and S. Y. Wu, J. Vac. Sci. Tech. 11, 130 (1974).

3. A. Gangulee, Acta Met. 22, 177 (1974).

4. R. W. Hoffman, in "Physics of Thin Films" (G. Hass and R. E. Thun, eds.), Vol. 3. Academic Press, New York (1966).

5. R. W. Hoffman in "Thin Films", H. G. F. Wilsdorf, ed. A.S.M. (1964).

6. D. S. Campbell, in "Basic Problems in Thin Film Physics" (R. Niedermayer and H. Mayer, eds.), p. 223. Vandenhoeck and Ruprecht, Göttingen (1966).

7. D. S. Campbell, in "Handbook of Thin Film Technology", (Maissel and Glang, eds.), p. 12-1. McGraw-Hill, New York (1970).

8. W. Buckel, J. Vac. Sci. Tech. 6, 606 (1969).

9. K. Kinosita, Thin Solid Films 12, 17 (1972).

10. R. J. Scheuerman, in "Symposium on Deposited Dielectric Thin Films", (F. Vratny, ed.), p. 561. Electrochemical Society, New York (1969).

11. See, for example: K. L. Chopra, "Thin Film Phenomena", McGraw-Hill, New York (1969) and, L. Maissel and M. H. Francombe, "Introduction to Thin Film Physics". Gordon and Breach, New York (1973).

12. J. F. Nye, "Physical Properties of Crystals", Oxford Univ. Press, London (1957).

13. C. S. Smith, in "Solid State Physics", Vol. 6, F. Seitz and D. Turnbull, eds. Academic Press, New York (1958).

14. R. W. Vook and F. Witt, J. Appl. Phys. 36, 2169 (1965).

15. J. Turley and G. Sines, J. Appl. Phys. 41, 3722 (1970).

16. T. Y. Thomas, Proc. Nat. Acad. Sci. (U.S.) 55, 235 (1966).

17. A. Brenner and S. Senderoff, J. Res. Natl. Bur. Stand. 42, 89 (1949).

18. F. A. Doljack, AEC Tech. Rept. 76, Case Western Reserve University, Cleveland, Ohio (1971).

19. E. Klokholm, in "X-ray Diffraction and Stress in Thin Films Symposium", IBM Thomas J. Watson Research Center, Yorktown Heights, New York (March 1969).

20. G. G. Stoney, Proc. Roy. Soc. (London) A32, 172 (1909).

21. P. Chaudhari, IBM J. Res. Develop. 13, 197 (1969).

22. H. J. Oel and V. D. Frechette, J. Am. Ceram. Soc. 50, 542 (1967).

23. J. Aleck, J. Appl. Mech. 16, 118 (1949).

24. K. Haruta and W. J. Spencer, J. Appl. Phys. 37, 2232 (1966).

25. R. W. Hoffman in "The Use of Thin Films in Physical Investigations", T. C. Anderson, ed. Academic Press, New York (1966).

26. R. W. Hoffman in "Measurement Techniques for Thin Films" Schwartz and Schwartz, eds. Electrochemical Society (1967).

27. D. G. Ashwell and E. D. Greenwood, Engineering 170, 51 (1950).

28. D. G. Bellow, G. Ford, and J. S. Kennedy, Exp. Mech. 227 (1965).

29. R. E. Rottmayer and R. W. Hoffman, J. Vac. Sci. Tech. 7, 461 (1970).

30. R. W. Springer, AEC Tech. Rept. 79, Case Western Reserve University, Cleveland, Ohio (1972).

31. J. D. Finegan and R. W. Hoffman, Trans. 8th Vacuum Symposium, p. 935. Pergamon Press (1962).

32. F. A. Doljack and R. W. Hoffman, Thin Solid Films 12, 71 (1972).

33. P. H. Robinson and D. J. Dumin, J. Electrochem. Soc. 115, 75 (1968).

34. P. M. Alexander, AEC Tech. Rept. 85, Case Western Reserve University, Cleveland, Ohio (1974).

35. K. Maki and K. Kinosita, Reported in K. Kinosita Proc. Second Colloquium on Thin Films, p. 31 (1967).

36. E. Yoda, J. Appl. Phys. Japan 8, 191 (1969).

37. E. Yoda, J. Appl. Phys. Japan 8, 1355 (1969).

38. Y. Namba, Oyo Buturi 38, 411 (1969)

39. R. E. Rottmayer, AEC Tech. Rept. 64, Case Western Reserve University, Cleveland, Ohio (1970).

40. R. W. Springer and R. W. Hoffman, J. Vac. Sci. Tech. 10, 238 (1973).

41. R. E. Rottmayer and R. W. Hoffman, J. Vac. Sci. Tech. 8, 152 (1971).

42. A. E. Ennos, Appl. Optics 5, 51 (1966).

43. A. Taloni and D. Hanneman, Surface Sci. 8, 323 (1967).

44. A. G. Blachman, Metallurg. Trans. 2, 699 (1971).

45. K. A. Haines and B. P. Hildebrand, Appl. Optics 5, 595 (1966).

46. R. J. Magill and T. Young, J. Vac. Sci. Tech. 4, 47 (1967).

47. R. Glang, R. A. Holmwood, and R. L. Rosenfeld, Rev. Sci. Instr. 36, 7 (1965).

48. N. N. Axelrod and H. J. Levinstein, unpublished.

49. F. P. Chiang, C. S. Faber, and F. Y Wang, J. Appl. Phys. 42, 1422 (1971).

50. J. W. Beams, in "Structure and Properties of Thin Films", C. A. Neogebauer, J. D. Newkirk, and D. A. Vermilyea, eds., p. 183. Wiley, New York (1959).

51. R. J. Jaccodine and W. A. Schlegel, J. Appl. Phys. 37, 2429 (1966).

52. C. H. Lane, IEEE Trans. Electron. Dev. ED-15, 998 (1968).

53. S.C.H. Lin and I. Pugacz-Muraszkiewicz, J. Appl. Phys. 43, 119 (1972).

54. C. W. Wilmsen, E. G. Thompson, and G. H. Meissner, IEEE Trans. Electron. Dev. ED-19, 122 (1972).

55. P. M. Schaible and R. Glang "Symposium on Deposited Dielectric Thin Films (F. Vratny, ed.), p. 577, Electrochemical Society, New York (1969).

56. G. Zosi, Z. Angew. Phys. 24, 322 (1968).

57. G. W. Bush and H. J. Read, J. Electrochem. Soc. 111, 289 (1964).

58. A. Taylor, "X-ray Metallography", Wiley, New York (1961).

59. T. I. Kamins and E. S. Meieran, J. Appl. Phys. 44, 5065 (1973).

60. B. D. Cullity, J. Appl. Phys. 35, 1915 (1964).

61. B. Borie, Acta Cryst. 13, 542 (1960).

62. B. Borie, C. J. Sparks, and J. V. Cathcart, Acta Met. 10, 691 (1962).

63. C. B. McDowell and T. C. Pilkington, J. Appl. Phys. 42, 2958 (1971).

64. A. Authier, "Proc. of the 15th Annual Conf. on Application of X-ray Analysis" (J. B. Newkirk and G. Mallet, eds.), (1967)

65. E. S. Meieran and I. A. Blech, J. Appl. Phys. 36, 3162 (1965).

66. I. A. Blech and E. S. Meieran, Appl. Phys. Letters 9, 245 (1966).

67. G. H. Schwuttke and J. K. Howard, J. Appl. Phys. 39, 1581 (1968).

68. P. Penning and D. Polder, Philips Res. Rept. 16, 419 (1961).

69. R. Zeyfang, J. Appl. Phys. 42, 1182 (1971).

70. G. A. Rozgonyi and T. J. Ciesielka, Rev. Sci. Instr. 44, 1053 (1973).

71. E. P. EerNisse, J. Appl. Phys. 43, 1330 (1972).

72. E. P. EerNisse, J. Appl. Phys. 44, 4482 (1973).

73. F. K. Reinhart and R. A. Logan, J. Appl. Phys. 44, 3171 (1973).

74. R. W. Vook and F. Witt, J. Vac. Sci. Tech. 2, 49 (1965).

75. R. Zeyfang, Solid State Electron. 14, 1035 (1971).

76. R. Feder and T. B. Light, J. Appl. Phys. 43, 3114 (1972).

77. H. Schlötterer, Solid State Electron. 11, 947 (1968).

78. A. J. Hughes and A. C. Thorsen, J. Appl. Phys. 44, 2304 (1973).

79. A. C. Thorsen and A. J. Hughes, Appl. Phys. Letters 21, 579 (1972).

80. A. J. Hughes (unpublished). To appear in J. Appl. Phys.

81. Y. Nakajima and K. Kinosita, Thin Solid Films 5, R5 (1970).

82. J. Stringer, Corrosion Sci. 10, 513 (1970).

83. F. N. Rhines and J. S. Wolf. Reported in Ref. 82.

84. C. J. Dell'Oca, D. L. Pulfrey, and L. Young, in "Physics of Thin Films" (M. Francombe and R. W. Hoffman, eds.)., Vol. 6. Academic Press, New York (1971).

85. L. Young, "Anodic Oxide Films", Academic Press, New York (1961).

86. D. A. Vermilyea, in "Advances in Electrochemistry", Vol. 3. Wiley (Interscience), New York (1963).

87. J. H. Van der Merwe, in "Single Crystal Films", (M. Francombe and H. Sato, eds.), Pergamon Press, Oxford (1964).

88. J. H. Van der Merwe and N. G. Van der Berg, Surface Sci. 32, 1 (1972).

89. J. H. Van der Merwe, Proc. 6th International Vacuum Congress (to be published).

90. J. W. Matthews, in "Physics of Thin Films" (G. Hass and R. E. Thun, eds.), Vol. 4. Academic Press, New York (1967).

91. J. W. Matthews, S. Mader, and T. B. Light, J. Appl. Phys. 41, 3800 (1970).

92. W. A. Jesser and D. Kuhlmann-Wilsdorf, J. Appl. Phys. 38, 5128 (1967).

93. W. A. Jesser and D. Kuhlmann-Wilsdorf, Phys. Stat. Sol. 19, 95 (1967).

94. K. Yagi, K. Takayanagi, K. Kobayashi, and G. Honjo, J. Cryst. Growth 9, 84 (1971).

95. R. Carpenter and D. S. Campbell, J. Mater. Sci. 2, 173 (1967).

96. P. J. Besser, J. E. Mee, P. E. Elkins, and D. M. Heinz, Mat. Res. Bull. 6, 1111 (1971).

97. J. R. Carruthers, J. Cryst. Growth 16, 45 (1972).

98. A. J. Braginski, T. R. Oeffinger, W. E. Kramer, D. K. McLain, and W. J. Takei, IEEE Trans. Mag., 8, 300 (1972).

99. N. Cabrera, Surface Sci. 2, 320 (1964).

100. C. Herring, "Structure and Properties of Crystal Surfaces", (R. Gomer and C. S. Smith, eds.), Univ. of Chicago Press, Chicago, Illinois (1953).

101. R. G. Linford and L. A. Mitchell, Surface Sci. 27, 142 (1971).

102. H. J. Wasserman and J. S. Vermaak, Surface Sci. 32, 168 (1972).

103. E. Ritter, to appear in Physics of Thin Films.

104. P. A. Young, Thin Solid Films 6, 423 (1970).

105. E. Klokholm and R. Berry, J. Electrochem. Soc. 115, 823, (1968).

106. S. Mader, J. Vac. Sci. Tech. 11, 131, (1974).

107. P. Chaudhari, J. Vac. Sci. Tech. 9, 520 (1972).

108. J. D. Wilcox, D. S. Campbell, and J. C. Anderson, Thin Solid Films 3, 13 (1969).

109. A. Yelon, J. R. Asik, and R. W. Hoffman, J. Appl. Phys. 33, 949 (1962).

110. D. O. Smith, M. S. Cohen, and G. P. Weiss, J. Appl. Phys. 31, 1775 (1960).

111. M. S. Abrahams, L. R. Weisberg, and J. J. Tietjen, J. Appl. Phys. 40, 3754 (1969).

112. K. Saito, R. O. Bozkurt, and T. Mura, J. Appl. Phys. 43, 182 (1972).

113. J. Reisenfeld and R. W. Hoffman, AEC Tech. Rept. 39, Case Institute of Technology, Cleveland, Ohio (1965).

114. A. F. Turner, "Thick Thin Films", Bausch & Bomb Tech. Rept. (1951).

115. O. S. Heavens and S. D. Smith, J. Opt. Soc. Am. 47, 469 (1957).

116. H. Blackburn and D. S. Campbell, in "Trans. 8th Nat. Vacuum Symp.", p. 943. Pergamon Press, Oxford (1961).

117. K. Kinosita, K. Nakamizo, K. Maki, K. Onuki, and K. Takenchi, J. Appl. Phys. Japan 4 (Suppl. 1), 340 (1965).

118. A. Barna, P. B. Barna, J. F. Pocza, and I. Pozsgai, Thin Solid Films 5, 201 (1970).

119. A. Preisinger and H. K. Pulker, private communication (to be published).

120. H. K. Pulker and E. Jung, Thin Solid Films 9, 57 (1971).

121. J. R. Priest, H. L. Caswell, and Y. Budo, J. Appl. Phys. 34, 347 (1963).

122. A. E. Hill and G. R. Hoffman, Brit. J. Appl. Phys. 18, 13 (1967).

123. D. J. Dumin, J. Appl. Phys. 36, 2700 (1965).

124. C. Y. Ang and H. M. Manasevit, Solid State Electron. 8, 994 (1965).

125. R. Zeyfang, J. Appl. Phys. 41, 3718 (1970).

126. W. A. Pliskin, in "Physics of Thin Films", (G. Hass and R. E. Thun, eds.), Vol. 4. Academic Press, New York (1967).

127. M. V. Whelan, A. H. Goemans, and L.M.C. Goossens, Appl. Phys. Letters 10, 262 (1967).

128. W. A. Westdorp and G. H. Schwuttke, in "Symposium on Deposited Dielectric Thin Films" (F. Vratny, ed.), p. 546. Electrochemical Society, New York (1969).

129. M. Tamura and H. Sunami, J. Appl. Phys. Japan 11, 1097 (1972).

130. M. J. Rand and J. F. Roberts, J. Electrochem. Soc.

131. H. Blackburn and D. S. Campbell, Phil. Mag. 8, 823 (1963).

132. Y. Doi, Machine Test. Lab Rept. (Japan) 27, 44 (1958).

133. D. M. Mattox and G. J. Kominiak, J. Electrochem. Soc. 120, 1535 (1973).

134. D. S. Campbell, "Trans. 9th Nat'l Vacuum Symp.", p. 29. The Macmillan Co., New York (1962).

135. A. Catlin and W. P. Walker, J. Appl. Phys. 31, 2135 (1960).

136. H. Schroder and G. M. Schmidt, Z. Angew. Phys. 18, 124 (1964).

137. J. Reisenfeld and R. W. Hoffman, AEC Tech. Rept. 39, Case Institute of Technology, Cleveland, Ohio (1965).

138. J. D. Wilcock, Ph.D. Thesis, Imperial College, London (1967).

139. L. Holland, T. Putner, and R. Ball, Brit. J. Appl. Phys. 11, 167 (1960).

140. M. A. Novice, Brit. J. Appl. Phys. 13, 561 (1962).

141. M. A. Novice, Vacuum 14, 385 (1964).

142. J. Priest, H. L. Caswell, and Y. Budo, "Trans. 9th Nat'l Vacuum Symp.", p. 121. The Macmillan Co., New York (1962).

143. J. D. Finegan and R. W. Hoffman, AEC Tech. Rept. 15. Case Institute of Technology (1961).

144. J. Priest, Rev. Sci. Instr. 32, 1349 (1961).

145. Y. Budo and J. Priest, Solid-State Electron. 6, 159 (1963).

146. J. Priest and H. L. Caswell, "Trans. 8th Nat'l Vacuum Symp.", p. 947. Pergamon Press, Oxford (1961).

147. R. J. Scheuerman, J. Vac. Sci. Tech. 7, 143 (1970).

148. H. Sunami, Y. Itoh, and K. Sato, J. Appl. Phys. 41, 5115 (1970).

149. J. A. Aboaf, J. Electrochem. Soc. 116, 1732 (1969).

150. A. G. Blachman, Mett. Trans. 2, 699 (1971).

151. A. G. Blachman, J. Vac. Sci. Tech. 10, 299 (1973).

152. R. J. Scheuerman, J. Vac. Sci. Tech. 6, 145 (1969).

153. W. Heitman, Appl. Optics 10, 2685 (1971).

154. P. R. Stuart, Vacuum 19, 507 (1969).

155. D. A. Vermilyea, J. Electrochem. Soc. 110, 345 (1963).

156. S. S. Lau and R. H. Mills, Phys. Stat. Sol. 17, 609 (1973).

157. L. Gmita and E. Teneseu, Rev. Roumaine Phys. 12, 79 (1967).

158. C. Drum and M. J. Rand, J. Appl. Phys. 39, 4458 (1968).

159. J. C. Grosspreutz, Surface Sci. 8, 173 (1967).

160. R. Lathlaen and D. H. Diehl, J. Electrochem. Soc. 116, 620 (1969).

161. R. Carpenter and D. S. Campbell, J. Mater. Sci. 4, 526 (1969).

162. C. Mai, S. Audision, and R. Riviere, C. R. Acad. Sci. Ser. B 269, 1185 (1969).

163. C. M. Drum, R. N. Tauber, J. D. Ashner, P. F. Schmidt, ABS Spring Mtg., Electrochemical Soc., Washington, D.C. (1971).

164. F. B. Micheletti and S. H. McFarlane, ABS Spring Mtg., Electrochemical Soc., Washington, D.C. (1971).

165. A. I. Vousi and L. P. Strakhov, Fiz. Tverd. Tela. 12, 3319 (1970).

166. M. Plassa, Thin Solid Films, 3, 305 (1969).

167. R. C. Sun, T. C. Tisone, and P. D. Cruzan, J. Appl. Phys. 44, 1009, (1973).

168. D. M. Mattox and G. J. Kominiak, J. Vac. Sci. Tech., 9, 528 (1972).

169. D. M. Mattox, 6th International Vacuum Congress, Kyoto, 1974 (to be published).

170. R. D. Bland, G. J. Kominiak and D. M. Mattox, J. Vac. Sci. Tech., 11, 671 (1974).

171. H. S. Story and R. W. Hoffman, Proc. Phys. Soc. B 70, 950 (1957).

172 N. S. Rasor and R. W. Hoffman, Phys. Rev. 98, 1555 (1955).

173. W. B. Pennebacker, J. Appl. Phys. 40, 394 (1969).

174. P. Chaudhari. Busmitted to J. Appl. Phys.

175. A. Gangulee, Phil. Mag., 17, 865, (1970).

176. W. J. Takei and M. H. Francombe, Solid State Electronics 11, 205 (1968).

177. S. S. Lau and R. C. Sun, Thin Solid Films, 10, 273 (1972).

178. R. R. Hart, D. H. Lee and O. J. Marsh, Appl. Phys. Letters 20, 76 (1972).

179. D. H. Lee, R. R. Hart and O. J. Marsh, Appl. Phys. Letters 20, 73 (1972).

180. International Conference on Low Temperature Diffusion and Applications to Thin Films. A. Gangulee, P. S. Ho, and K. N. Tu, Yorktown Hts., (1974). To be published in Thin Solid Films.

181 R. S. Blewer and J. K. Maurin, J. Nec. Mat., 44, 260 (1972).

182. B. S. Berry and W. C. Pritchet, J. Appl. Phys., 44, 3122 (1973).

183. H. Biehl and H. H. Mende, J. Phys. Chem. Solids, 35, 37 (1974).

184. S. Spinner, J. Am. Ceram. Soc., 37, 229 (1954).

185. S. Spinner, J. Am. Ceram. Soc., 38, 113 (1955).

186. K. Uozumi, T. Nakada and A. Kinbara, Thin Solid Films, 12, 67 (1972).

187. H. S. Chen and T. T. Wang, J. Appl. Phys. 41, 5338 (1970).

188. S. I. Tan, B. S. Berry, and B. L. Crowder, App. Phys. Letters 20, 88 (1972).

189. R. F. Bunshah, J. Vac. Sci. Tech., 11, 633 (1974).

190. Conference on Structure/Property Relationships in Thick Films/ and Bulk Coatings, J. Vac. Sci. Tech. 11, (1974).

191. R. E. Winter, Thin Solid Films, 12, 81 (1972).

192. R. A. Hunt and B. Gale, J. Phys. D Appl. Phys., 5, 359 (1972).

193. R. C. Sundahl, J. Vac. Sci. Tech., 9, 181 (1972).

194. A. Yelon and O. Voegeli, in Single Crystal Films, M. Francombe and H. Sato, eds., p. 321. Pergamon Press, Oxford (1964).

195. K. H. Behrndt, J. Vac. Sci. Tech., 2, 63 (1965).

196. J. W. Matthews and F. Klokholm, Mat. Res. Bull., 7, 213 (1972).

197. J. W. Matthews, E. Klokholm, and T. S. Plasket, IBM J. Res. Develop., 17, 426 (1973).

198. Aspects of Adhesion, D. J. Alner, ed. U. of London Press, London (Multiple Volumes).

199. H. Krupp, Adv. Colloid Interface Sci., 1, 111 (1967).

200. J. Ferrante and J. R. Smith, Surface Sci., 38, 77 (1973).

201. N. L. Harrison and W. J. Harrison, J. Adhesion, 3, 195 (1972).

202. B. N. Chapman, J. Vac. Sci. Tech. 11, 106 (1974).

203. K. Kendall, J. Adhesion 5, 179 (1973).

204. C. Weaver, to be published.

205. D. M. Mattox, J. Vac. Sci. Tech., 10, 47 (1973).

206. C.T.H. Stoddart, D. R. Clarke, and C. T. Robbie, J. Adhesion 2, 270 (1970).

207. J. E. Houston and R. D. Bland, J. Appl. Phys., 44, 2504 (1973).

208. W. D. Westwood and C. D. Bennewitz, Private Communication. (To be published.)

209. R. C. Sun, T. C. Tisome and P. D. Cruzan. Private communication. (Submitted for publication in J. Appl. Phys.)

210. I. J. Hodgkinson and A. R. Walker, Thin Solid Films 17, 185 (1973).

211. M. D. Merz, R. P. Allen and S. D. Dahlgren, J. Appl. Phys. 45, 4126 (1974).

212. D. Weaire, M. F. Ashby, J. Logan and M. J. Weins, Acta Metall. 19, 779 (1971).